Anti-Pyruvate Dehydrogenase Complex Autoantibodies in Patients with Suspected Autoimmune Encephalitis

Doctoral thesis

to obtain a doctorate (Dr. med.)

from the Faculty of Medicine

of the University of Bonn

Chiara Adina Hummel

from Ravensburg

2026

Written with authorization of

the Faculty of Medicine of the University of Bonn

First reviewer: Prof. Dr. med. Albert Johann Becker

Second reviewer: Prof. Dr. med. Anne-Kathrin Pröbstel

Day of oral examination: 01/16/2026

From the Institute of Neuropathology

Table of contents

List of Abbreviation

AB	Antibody
AE	Autoimmune Encephalitis
ASM	Antiseizure Medication
AMAs	Antimitochondrial Autoantibodies
AMPAR	α-Amino-3-hydroxy-5-methyl-isoxazolepropionic acid Receptor
AMPH	Amphiphysin
ANAs	Antinuclear Antibody
AutoAB	Autoantibody
APS	Antiphospholipid syndrome
BSA	Bovine serum albumin
CA	Cornu Ammonis
CASPR2	Contactin-associated protein-like 2
cDNA	complementary DNA
cMRI	cerebral Magnetic Resonance Imaging
CSF	Cerebrospinal fluid
Ctrl.	Control
DAPI	2-Phenylindol
DIV	day in vitro
DLAT	Dihydrolipoyllysine-residue acetyltransferase (E2)
DLD	Dihydrolipoamide dehydrogenase (E3)
DLG2	Discs large MAGUK scaffold protein 2
FLAIR	fluid-attenuated inversion recovery
GABAbR	metabotropic Gamma-Aminobutyric Acid Receptor
GAD65	Glutamate-Decarboxylase Isoform 65
h	hours
HEK	Human embryonal kidney

HS	Hippocampal Sclerosis
IP	Immunoprecipitation
KCNC3	Potassium voltage-gated channel subfamily C member 3
kDa	Kilodalton
LE	Limbic Encephalitis
LGI1	Leucine-rich Glioma Inactivated Protein 1
min	minutes
MM	Mitochondrial Membrane
MS	Mass Spectrometry
NGS	Normal goat serum
NMDAR	N-Methyl-D-Aspartate-Receptor
Pat.	Patient
PBC	Primary Biliary Cholangitis
PBS	Phosphate-buffered saline
PDH	Pyruvate Dehydrogenase
PDHc	Pyruvate Dehydrogenase complex
PDCD	Primary PDH complex deficiency
PFA	Paraformaldehyde
PHNs	murine Primary hippocampal neurons
PKP4	Plakophilin 4
s	Serum
SDS-PAGE	Sodium Dodecyl Sulfate – PolyAcrylamid Gel Electrophoresis
SLE	Systemic lupus erythematosus
SOX1	SRY-box transcription factor 1
SS	Systemic sclerosis
TLE	Temporal lobe epilepsy
TX-100	Triton X-100

1. Introduction

1.1 Autoimmune encephalitis as epileptic syndrome

The spectrum of autoimmune encephalitis (AE) is a progressive immune-mediated disease that causes inflammation in the brain, characterized by limbic and extra-limbic dysfunction (Gole and Anand, 2025; Leypoldt et al., 2013). A diagnosis of limbic encephalitis (LE) can be made when specific criteria related to limbic impairment are met (Graus et al., 2016). AE is increasingly recognized as a major cause of adult-onset temporal lobe epilepsy (TLE) (Bien et al., 2007). Patients typically experience severe epileptic seizures, including focal to bilateral tonic-clonic seizures, which are often refractory to antiseizure medication (ASM). Additionally, short-term memory deficits, altered mental status and psychiatric symptoms are commonly reported (Leypoldt et al., 2013). On cerebral magnetic resonance imaging (cMRI), T2-weighted fluid-attenuated inversion recovery (FLAIR) sequences often show hyperintense signals in the medial temporal lobes, including the hippocampus and amygdala, although these abnormalities can sometimes extend beyond the temporal lobes or can even be absent (Heine et al., 2015). Cerebrospinal fluid (CSF) analyses often show pleocytosis or elevated protein concentration, while brain biopsies can reveal a spectrum of inflammation, ranging from primarily lymphocytic infiltration of the limbic structures to hippocampal sclerosis (HS) (Bauer and Bien, 2016; Pitsch et al., 2020). The exact mechanisms driving AE remain unclear, but in recent decades specific autoantibodies (autoABs) have been identified that target neuronal structures within the central nervous system (CNS) (Dalmau and Graus, 2018; Geis et al., 2019; Kao et al., 2021). These autoABs target either neuronal surface proteins or intracellular antigens. Surface antigen targets include synaptic plasma membrane proteins, like receptor-gated ion channels such as the N-methyl-D-aspartate-receptor (NMDAR) (Dalmau et al., 2007), the α-amino-3-hydroxy-5-methyl-isoxazolepropionic acid receptor (AMPAR) (Lai et al., 2009), neurotransmitter receptors such as the metabotropic gamma-aminobutyric acid receptor (GABAbR) (Lancaster et al., 2010) or voltage-gated potassium channel-associated proteins, including the leucine-rich glioma inactivated protein 1 (LGI1) (Lai et al., 2010) and contactin-associated protein-like 2 (CASPR2) (Lancaster et al., 2011). In contrast, intracellular autoABs target proteins such as amphiphysin (AMPH), the presynaptic protein glutamate decarboxylase isoform

65 (GAD65), or various intranuclear antigens, including the human neuronal RNA-binding protein Hu, the paraneoplastic antigen Ma2/Ta, the Purkinje cell antigen 1 Yo and the anti-SRY-box transcription factor (SOX1) (Dalmau and Rosenfeld, 2008; Darnell and Posner, 2003; Graus et al., 2010; Malter et al., 2010). Interestingly, however, a specific autoAB is only found in a small proportion (13%) of clinically suspected AE patients (Brenner et al., 2013; Kuehn et al., 2020; von Podewils et al., 2017), ranging from 3% for anti-LGI1 or anti-AMPH to 46% for anti-GAD65. The other 87% of patients are found to be seronegative for known autoABs. Several screening tests for unknown autoABs such as immunoblotting with brain lysate or brain sections, and indirect immunofluorescence tests reveal that 25 % of patients with suspected AE are found to be positive for autoABs binding to brain-reactive proteins (Kuehn et al., 2020). This suggests that many seronegative AE patients may hold so far unidentified autoABs, indicating significant gaps in our current understanding of AE.

In exploring the pathogenic mechanisms of autoABs, it is important to distinguish between those that target intracellular antigens and those that target surface antigens. AutoABs against neuronal surface antigens are generally believed to have a direct pathogenic effect. They can interact with cell surface receptors, disrupting their function by promoting their internalization, which leads to abnormal neuronal activity. The resulting brain immunopathology is often driven by humoral or complement-mediated immune response, characterized by intrathecal autoAB production (Bien et al., 2012; Zhang et al., 2013). In contrast, intracellular autoABs may be associated with paraneoplastic syndromes and the pathogenic effect is likely to be mediated by cytotoxic T cells rather than the autoABs themselves (Bien et al., 2012). Therefore, intracellular autoABs are considered biomarkers rather than direct mediators of pathology (Bien and Scheffer, 2011). Nevertheless, a novel autoAB targeting the intracellular postsynaptic scaffolding protein Drebrin has recently been identified, marking the first AE-associated autoAB that appears to have functional significance despite targeting an intracellular antigen (Pitsch et al., 2020). Drebin plays a role in dendritic spine morphology, and anti-Drebin autoAB have been shown to impair synaptic structures and promote hyperexcitable neuronal networks in vitro (Pitsch et al., 2020). However, the underlying cellular mechanisms remain poorly

understood, and further research into the pathogenic mechanisms of AE-associated autoABs is needed.

In summary, AE is a serious and complex disease spectrum, for which our current understanding of its pathogenesis remains incomplete, and its diagnosis can be challenging. Accurate and timely diagnosis is crucial because of the direct therapeutic implications. Given the autoimmune nature of AE, immunosuppressive therapy remains the mainstay of treatment, although patients with autoABs against surface antigens tend to respond better than those with intracellular autoABs (Bien, 2022; Tüzün and Dalmau, 2007). The further identification of relevant autoABs is crucial to improve AE diagnostic approaches. Furthermore, the characterization of autoABs is of significant clinical interest, as a deeper understanding of their pathological mechanisms will help identify disease mechanisms, which is essential for the development and optimization of potential targeted therapies. Given the high prevalence of seronegative patients suspected of having AE who test positive for undefined brain-reactive autoABs, the identification of potential AE-associated autoABs appears to be a promising area for advancing both diagnostic and therapeutic strategies.

1.2 Identification of neuronal antigens

To identify potential AE-associated autoABs, antigens of brain protein-reactive autoABs from respective patients' sera or CSF need to be extracted and analyzed. This step is critical and so far, several methods have been described (Fig.1A). One option is to screen patient sera using commercial protein microarrays containing thousands of recombinant neuronal proteins, although this approach can be costly (Jarius et al., 2010) (Fig. 1A, a). A more common alternative is immunoprecipitation (IP) followed by mass spectrometry (MS). For example, complementary DNA (cDNA) libraries can be expressed in phages, transferred onto nitrocellulose filters, and subsequently incubating with patient sera to identify AB-bound antigens (Bataller et al., 2003; Quertermous, 2001) (Fig. 1A, b). A frequently used method to identify surface antigens, involves hippocampal neuron cultures that are fixed and incubated with patient sera (Lai et al., 2010; Lai et al., 2009) (Fig. 1A, c). However, preparing and culturing neurons from murine embryos is complex and time-consuming, limiting its use for a large screening (Scharf et al., 2018). To target both surface and intracellular proteins, IP can also be performed on cryopreserved murine

brain slides (Fig. 1A, d). After incubating sera with these slides, immunocomplexes are extracted to eliminate nonspecific proteins (Scharf et al., 2018). Nevertheless, differences in extractability from tissue sections may require using murine brain lysate as an alternative source (Scharf et al., 2018) (Fig. 1A, e). Across all IP approaches, the final step typically involves pulling down immunocomplexes with protein G beads, separating them via Sodium Dodecyl Sulfate – PolyAcrylamid Gel Electrophoresis (SDS-PAGE), and analyzing visually striking protein bands using MS (Lai et al., 2009; Scharf et al., 2018).

IP with murine brain lysate (Fig. 1A, e) is widely used and an effective method for identifying neuronal autoABs in seronegative AE patients, as demonstrated by Pitsch et al., 2020. However, the crucial step in this process is ensuring optimal solubilization of potential autoAB targets from brain tissue, preventing protein loss during extraction. Gleichman et al. (2012), and later Pitsch et al. (2020), used Triton X-100 (TX-100) as the detergent for solubilizing proteins. Furthermore, ComplexioLyte (CL) ready-to-use buffers from Logopharm, particularly CL 47 and CL 91, have been widely used in various studies to analyze different neuronal proteins in murine brain lysates, such as AMPAR complexes (Brechet et al., 2017), voltage-gated channels (Müller et al., 2010), membrane-associated proteins (Schmidt et al., 2017), and intracellular antigens, including mitochondrial proteins (Müller et al., 2016). Logopharm buffers are optimized for solubilizing membrane proteins and complexes from central and peripheral nervous system tissue, making them ideal for gel electrophoresis and affinity purification coupled with MS. Notably, Logopharm offered results from assays using affinity purification and MS to quantify AMPAR interaction partners with various lysis buffers. Their heat map (Fig. 1B) illustrates the MS-based quantification of membrane proteins with CL 47, CL 91, and TX-100, with CL 47 demonstrating the broadest range of protein detection (Logopharm GmbH, 2017; *data were obtained from the company in 2021 but are not publicly available*).

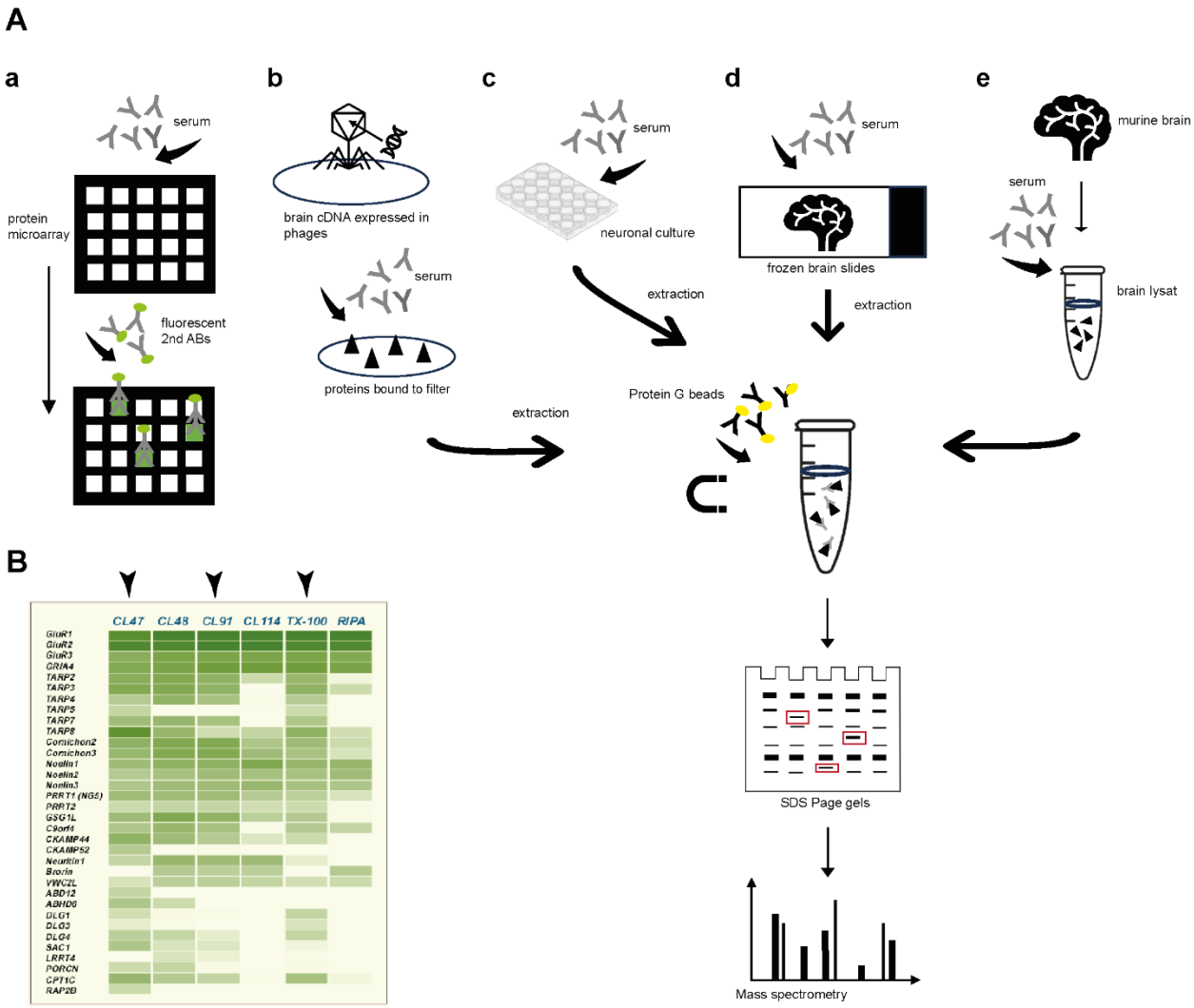

Fig. 1: Overview of methods for identification of neuronal antigens. (A) Antigens can be discovered by screening patient sera with (a) protein microarrays containing thousands of neuronal antigens or by IP followed by MS (b – e). (b) Neuronal cDNA libraries expressed in phage are immunoscreened, (c) patient sera are incubated with cultured hippocampal neurons, (d) cryopreserved mouse brain sections, or (e) mouse brain lysate. Immunocomplexes are pulled down with Protein G beads, separated by SDS-PAGE, and visually prominent protein bands are analyzed by MS. (B) Comparison of solubilization buffers, adapted from Logopharm GmbH, 2017 (*internal documentation*). Affinity purification and MS analysis were used to quantify AMPAR interaction partners, comparing different lysis buffers, including CL 47, CL 91, and TX-100 (arrows). The heat map shows representative MS-based quantification of membrane proteins, with CL 47 providing the broadest range of protein detection. *Created with Adobe Illustrator, 2021 and Microsoft PowerPoint 365.*

1.3 Anti-mitochondrial autoantibodies

Antimitochondrial autoantibodies (AMAs) were first reported by Walker et al. (1965) in sera of patients with primary biliary cholangitis (PBC). Since then, AMAs have been detected in a number of other autoimmune diseases, including systemic sclerosis (SS), Sjögren's syndrome, systemic lupus erythematosus (SLE), antiphospholipid syndrome (APS), and inflammatory myositis. They are also present in < 1% of healthy individuals (Colapietro et al., 2022; Favoino et al., 2023; Pisetsky et al., 2020). To date, nine types of AMAs have been identified, classified as anti-M1 to anti-M9, all of which are located in the inner or outer mitochondrial membrane (MM) or in the intermembrane space. Each subtype is associated with different disease groups, including infectious, collagenous, autoimmune or drug-induced diseases (Andrejevic et al., 2007; Berg et al., 1989; Grob et al., 1975; La Rosa et al., 1998; Timbrell, 1979) (see Fig. 2 for more details). Of these, PBC is considered the most sensitive as 95% of patients present positive for AMAs (Kumagi and Heathcote, 2008). It is an autoimmune disease characterized by chronic, progressive cholestasis in the liver, with degeneration and necrosis of intrahepatic biliary epithelial cells, leading to non-suppurative cholangitis, fibrosis, and potentially liver cirrhosis and hepatocellular carcinoma (Colapietro et al., 2022; Tanaka, 2021). AMAs are found in up to 95% of PBC patients and are highly regarded as biomarkers, although some functional research is ongoing (Colapietro et al., 2022; Houri and Hirschfield, 2024). Berg and Klein (1992) classified the AMA antigenic targets in PBC into four types: M2, M4, M8, and M9. Anti-M2 is considered the primary autoAB, targeting various enzymes in the inner MM (M2a – M2e), particularly the mitochondrial α-ketoacid dehydrogenase complex family, with a focus on the pyruvate dehydrogenase (PDH) complex. The roles of anti-M4, anti-M8, and anti-M9 remain controversial. Some data suggest that M4 and M8 may not represent distinct targets but may be artefacts, and the prognostic significance of specific AMA profiles appear to be unsubstantiated (Colapietro et al., 2022; Joshi et al., 2002; Palmer et al., 1993; Rigopoulou and Bogdanos, 2023; Davis et al., 1992).

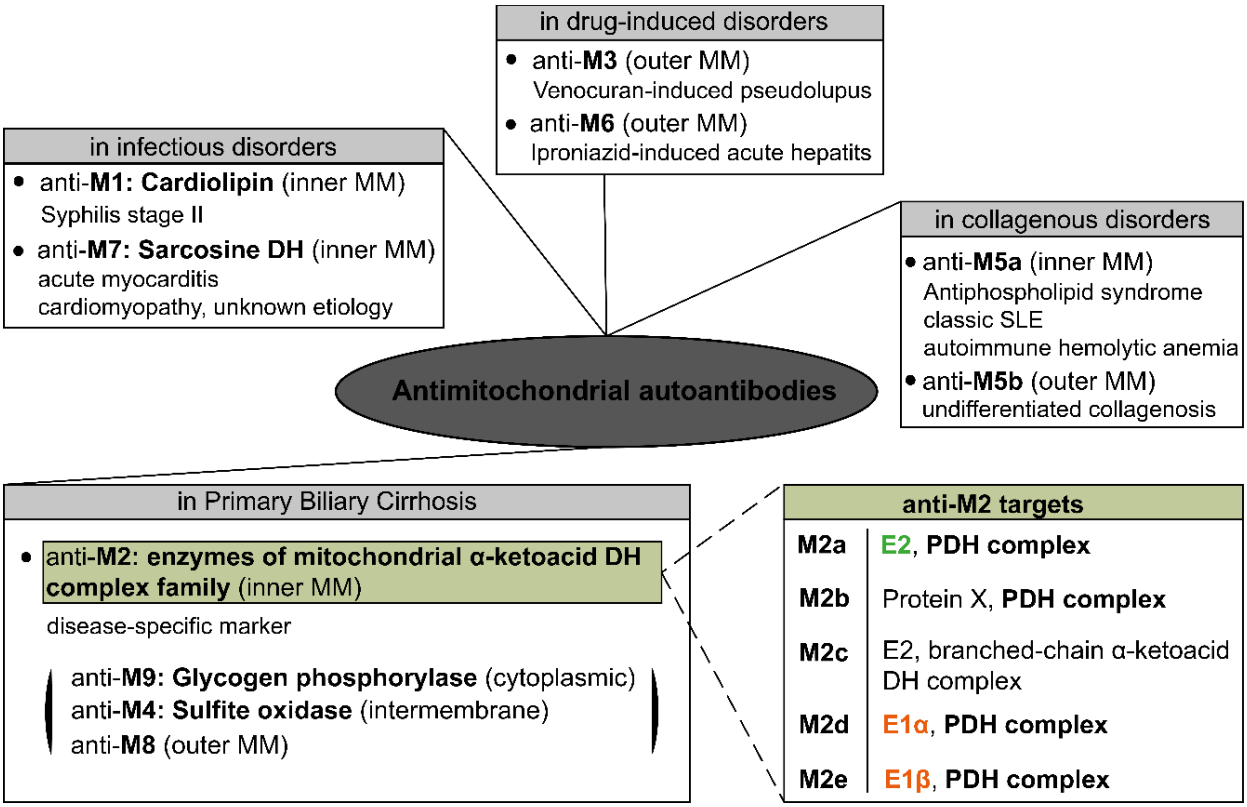

Fig. 2: Overview of the various target structures of AMAs and their classification into different disease groups. Presence of anti-M9, anti-M4, and anti-M8 are discussed controversy. MM – mitochondrial membrane. DH – Dehydrogenase. *Created with Adobe Illustrator, 2021.*

1.4 Pyruvate dehydrogenase complex

The PDH complex (PDHc), located in the inner MM of nucleated human cells, plays a critical role in energy metabolism, by linking glycolysis to the citric acid cycle through the conversion of pyruvate to acetyl-CoA (Stacpoole and McCall, 2023). Given its central role in energy production, the PDHc has a major impact on the CNS function, which has high metabolic demands (Patel et al., 2014; Stacpoole and McCall, 2023). Impairment of the PDHc due to mutations in its enzymes or cofactors, restricts aerobic respiration, leading to lactic acid accumulation and potential neuronal damage. Primary PDH complex deficiency (PDCD) is often associated with neurological symptoms, including developmental delay, hypotonia, epilepsy, and cerebral atrophy (Ganetzky et al., 2021).

As a member of the mitochondrial α-ketoacid dehydrogenase complex family, the PDHc shares the oxidative decarboxylation process with the α-ketoglutarate dehydrogenase

complex (responsible for the conversion of α-ketoglutarate to succinyl-CoA in the citric acid cycle) and the branched-chain α-ketoacid dehydrogenase complex (involved in the catabolism of branched-chain amino acids). This three-stage oxidative decarboxylation process requires five coenzymes: Thiamin pyrophosphate (TPP), lipoic acid, flavin adenine dinucleotide (FAD), oxidized nicotinamide adenine dinucleotide (NAD+), and coenzyme A (Berg et al., 2020).

The PDHc consists of three core subunits: E1, pyruvate dehydrogenase (E1α, ~43.2kDa and E1β, ~38.9kDa), which catalyzes pyruvate decarboxylation (Patel et al., 2014; Sgrignani et al., 2018); E2, dihydrolipoyllysine-residue acetyltransferase (DLAT, ~67.9kDa), which produces acetyl-CoA (Patel et al., 2014); and E3, dihydrolipoamide dehydrogenase (DLD, ~54kDa), which regenerates lipoate, by producing FADH2 and NADH (Patel et al., 2014; Patel et al., 2009). The E3 binding protein (E3BP), also called protein X, binds E3 to the complex (Ciszak et al., 2006; Patel et al., 2014) (Fig. 3).

In PBC, the E2 subunit of the PDHc (M2a) is the primary target of the anti-M2 AMAs, with E3BP (M2b), E1α (M2d), and E1β (M2e) also recognized as autoantigens (Fig. 2) (Berg and Klein, 1992; Leung et al., 1997; Poyatos et al., 2021; Rigopoulou and Bogdanos, 2023; Shuai et al., 2017).

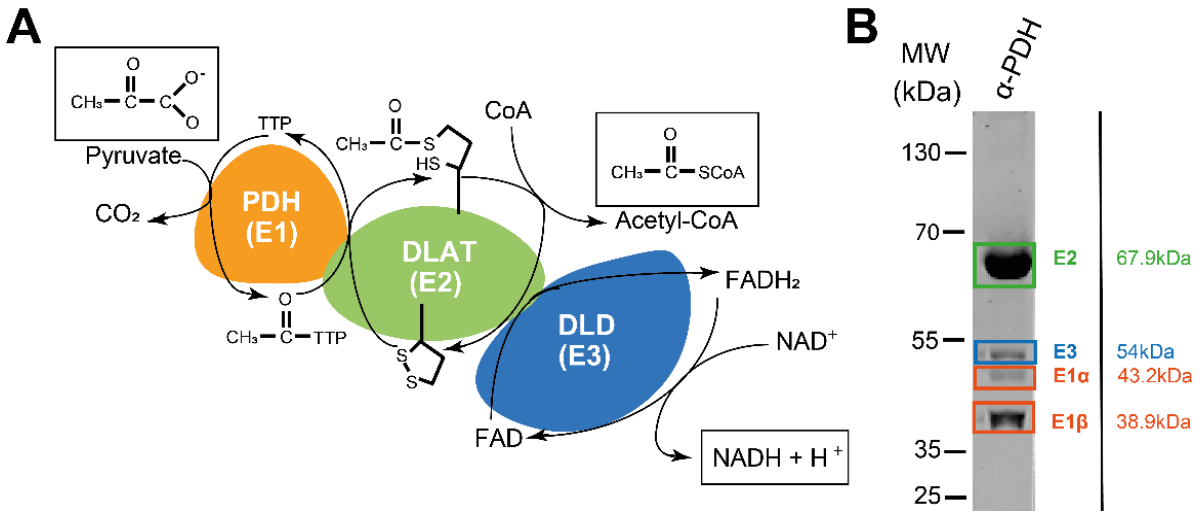

Fig. 3: Scheme of the PDHc and its subunits. (A) Composition of PDHc showing the interactions of the E1, E2, and E3 subunits, along with the corresponding chemical reactions of oxidative decarboxylation that converts pyruvate into acetyl-CoA, a key step in the initiation of the citric acid cycle. (B) Immunoblot of porcine heart PDHc showing the sizes of the different subunits detected by commercial monoclonal ABs targeting all subunit proteins. *Created with Adobe Illustrator, 2021.*

1.5 Objective targets

The main aim of this thesis is to analyze seronegative biosamples of patients with clinical suspicion of having AE who have been tested negative for known AE-associated autoABs but who presented positive screenings for brain protein- reactive ABs to assess possible underlying connections within this patient group by focusing on potential so far unidentified brain protein-reactive autoABs. This will provide insight into disease mechanisms, improve diagnostic procedures, and help to develop potential targeted therapies in AE in the future.

The first goal is to optimize the process of identifying putative targets of brain protein-reactive autoAB. This will involve the improvement of various methods, such as IP with solubilization of synaptic proteins from brain lysate. The identification of putative protein bands containing potential so far unidentified autoAB targets is a critical step. Additionally, effective handling of control samples and conducting a thorough evaluation of MS results

are essential. These improvements aim to refine the process and increase the accuracy of autoAB detection.

The second objective is to identify novel so far unidentified brain protein-reactive autoABs in biosamples of seronegative patients suspected of having AE by implementing the optimized assays. Once a specific target of a brain protein-reactive autoAB is identified by MS, the finding will be confirmed by specific Western blots. The study will then be extended to a larger cohort to assess the prevalence of this autoAB in seronegative patients with suspected AE at the University Hospital Bonn. Based on this, clinical data will be analyzed to correlate various patient characteristics, such as seizure semiology, cMRI imaging, CSF findings, neuropsychological abnormalities, and therapeutic response. This comprehensive approach will help to understand the clinical significance of this brain protein-reactive autoAB in AE.

The third objective is to characterize the specific identified autoAB and its target using several in vitro assays. This includes the investigation of the cellular and regional localization of the target protein in neuronal cultures and brain slices, which is a fundamental basis for elucidating the pathogenic mechanisms of autoABs in AE.

In conclusion, this thesis aims to significantly improve the understanding of seronegative patients who are suspected of AE and who screened positive for potential brain protein-reactive ABs by analyzing potential so far unidentified autoABs in patients' sera, by validating the presence in a seronegative AE patient cohort, by analyzing autoABs' and antigens' morphological characteristics and by interpreting the possible clinical and pathological significance. These results may contribute to a better understanding of pathological mechanisms and better diagnostic strategies in AE which is essential for developing and optimizing potential targeted therapies in the future.

2. Materials and Methods

2.1 Patients

This study included sera and if available CSF from 387 patients with seizures of unknown etiology from the University Hospital Bonn, Germany, collected between 2017 and 2021 (n (male) = 201, n (female) = 186; median age 51, 25 % percentile 33, 75 % percentile 62). In all patients AE has been a differential diagnosis based on their clinical symptoms and all were tested seronegative for known autoABs. However, sera of included patients showed strong additional bands on immunoblot screening, suggesting that they may be positive for unidentified brain protein-reactive autoABs (seronegative, screening-positive). All experiments adhered to the Declaration of Helsinki, and written informed consent was obtained from all patients according to the approvals of the local ethics committee of the University Hospital Bonn, Germany (Nr. 222/16, 229/18, 371/20, 504/20).

2.2 Control cohort

Six controls were used for the IP and MS, including samples from three healthy individuals and three seronegative patients suspected of having AE, but who showed no additional bands in immunoblot screening tests. For the immunoblot screening for anti-PDHc autoAB positive patients, controls consisted of sera from 31 healthy individuals (n(male) =14, n(female) =17; median age 28, 25 % percentile 27, 75 % percentile 43) showing no reactivity in immunoblot screening, CSF from three seronegative patients suspected of having AE but showing no additional bands, and sera from 100 seronegative patients suspected of having AE (n(male) =54, n(female) =46; median age 47.5, 25 % percentile 30, 75 % percentile 60.5) showing no additional bands were used. Control samples were analyzed in the same way as the sera from anti-PDHc autoAB positive patients.

2.3 Screening tests

2.3.1 - for known neuronal autoantibodies

All biospecimen from patients clinically suspected of having AE were screened for known antineuronal autoABs associated with neurological disease. Two different methods were used. For the detection of autoABs against intracellular antigens (AMPH, CV2, Ma2/Ta, RI, Ya, Hu, recoverin, SOX1, titin, ZIC4, GAD65 and Tr) a semiquantitative immunoblot (EUROLINE PNS 12, Euroimmun, DL 1111-1601-7 G) was used. For detection of

autoABs against neuronal surface proteins (NMDAR, CASPR2, LGI1, GABAaR, GABAbR, AMPAR) and GAD65 an indirect immunofluorescence assay based on human embryonic kidney (HEK) 293 cells with surface overexpression of the corresponding antigens (IIFT: 'Autoimmune encephalitis mosaic1', Euroimmun, FA 1120-1005-1; GAD65-IIFT, Euroimmun, FA 1022-1005-50) was used. These diagnostic assays were performed according to the manufacturer's instructions.

2.3.2 - for non-specific brain protein-reactive autoantibodies

Immunoblots were used to screen for putative brain protein-reactive autoABs in serum and CSF of patients who were initially seronegative (study design see Fig. 4). Brain protein lysates were prepared form patients with pharmacoresistant TLE (surgical resection for seizure relief), rat (Wistar) and mouse (C57BL/6N) whole brain, and murine crude synaptosomes. Proteins were denaturized using 6x Laemmli buffer (Laemmli, 1970), separated by electrophoresis, and transferred onto nitrocellulose membranes. After blocking with 2 % bovine serum albumin (BSA) (Roth, 8076.3), 2 % fetal calf serum (FCS), and 0.2 % cold water fish gelatin in phosphate-buffered saline (PBS), proteins were incubated overnight at 4°C with serum (diluted 1:500) or CSF (diluted 1:100). Membranes were washed multiple times with PBS/Tween 20 before and after being incubated for 45 minutes (min) with IRDye 800CW goat anti-human IgG ABs (Odyssey, 926-32232). Images were taken using Odyssey Imaging System (LI-COR). The immunoblot assay was considered positive if strong additional bands were visible which were not detectable in controls, indicating presence of brain protein-reactive autoABs.

2.4 Immunoprecipitation and mass spectrometry

IP was performed as recently described (Pitsch et al., 2020, PMID: 32196746) (study design see Fig. 4). Briefly, 1 g of freshly prepared whole mouse brain tissue was dissected and homogenized in 5 ml ComplexioLyte buffer 47a (Logopharm, CL-47a-05) with added protease inhibitor (Sigma-Aldrich, P8340-1ML). Lysate was rotated for 3 hours (h) at 4 °C. After centrifugation for 15 min at 4 °C and 21.000 x g, the supernatant was centrifuged in an ultracentrifuge for 30 min at 4 °C and 70.000 x g. The supernatant was incubated with serum overnight at 4 °C before being rotated with Dynabeads Protein G (ThermoFisher, 10004D) at 4 °C for 3 h. Dynabeads were washed three times with ComplexioLyte buffer 47a containing additional protease inhibitor. Samples were heated at 70 °C for 10 min with

NuPage LDS buffer 4x (ThermoFisher, NP0007) containing 0.25 M dithiothreitol for reduction of disulfide bridges. Then, 0.65 M iodacetamide was added. SDS-PAGE was performed using NuPAGE 4 to 12 %, Bi-Tris, 1.5 mm Mini-Proteins-Gels (ThermoFisher, NP0335) and NuPAGE MOPS SDS running buffer 20x (ThermoFisher, NP0001).

Biosamples were prepared in duplicates. After electrophoresis gels of the first replicate (replicate 1) were stained with Roti-Blue 5x (Roth, A152.1) to visualize protein bands. The second replicate (replicate 2) was blotted onto nitrocellulose membranes overnight. Membranes were blocked with 2 % BSA (Roth, 8076.3), 2 % fetal bovine serum (FBS) (Gibco, 10270-106), and 0.2 % cold water fish gelatin (Sigma, 67041.500G) in PBS before being cut into single lanes so each biosample could be incubated with its own serum (diluted 1:100 in mentioned buffer) at 4 °C overnight. Membranes were washed three times with TTBS (3 % NaCl, 0.25 % Tris, 0.5 % Tween20 in PBS) prior to incubation with goat anti-human IRDye 800CW (Odyssey, 926-32232) (diluted 1:20.000) for 1 hour, followed by further three washing steps. Signals of additional protein bands compared to healthy controls were visualized with the Odyssey Imaging System (LI-COR). Additional bands detected on western blot membranes (replicate 2) were cut out from corresponding stained gels (replicate 1). Gel fragments were transferred to MS (in collaboration with Prof. Gieselmann and Dr. Sylvester, Institute for Biochemistry and Molecular Biology, Univsersity of Bonn) where the contained proteins were digested by trypsin prior to protein identification. In the subsequent analysis, the measured abundance of every protein identified in a specific band of one patient was divided by the abundance of the same protein in matched control patients. The abundance and the ratio of abundance (patient/ control) was evaluated.

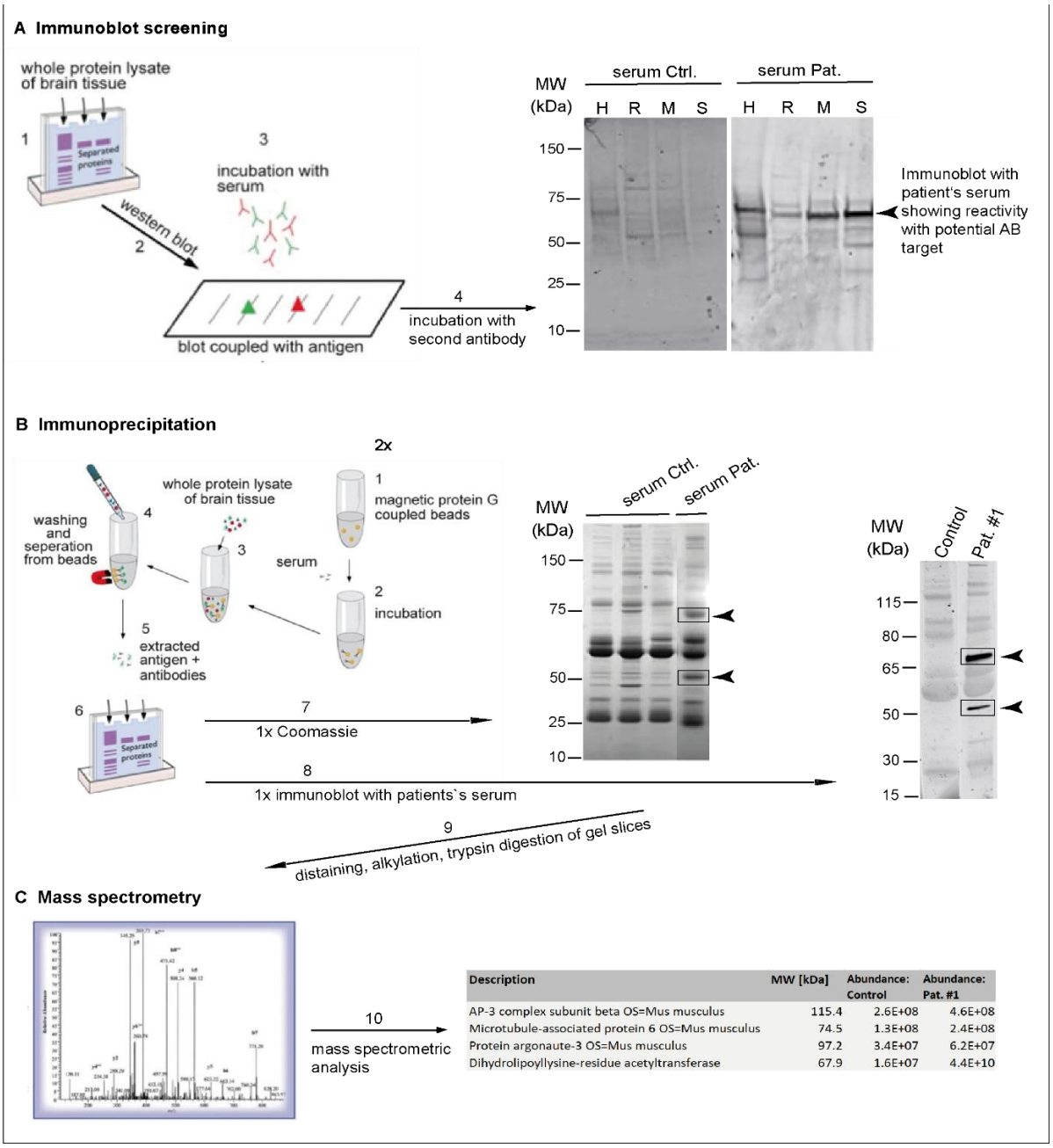

Description	MW [kDa]	Abundance: Control	Abundance: Pat. #1
AP-3 complex subunit beta OS=Mus musculus	115.4	2.6E+08	4.6E+08
Microtubule-associated protein 6 OS=Mus musculus	74.5	1.3E+08	2.4E+08
Protein argonaute-3 OS=Mus musculus	97.2	3.4E+07	6.2E+07
Dihydrolipoyllysine-residue acetyltransferase	67.9	1.6E+07	4.4E+10

Fig. 4: Scheme of screening for brain protein-reactive autoABs in seronegative patients and identification of their antigen targets. (A) Whole protein lysate from human (H), rat (R), and mouse brain tissue (M), as well as mouse brain synaptosomes (S) underwent SDS-PAGE and blotted membranes are incubated with seronegative patients' sample to allow any present autoABs to bind to their specific antigens followed by visualizing additional bands. (B) Samples from patients with strong additional bands in immunoblot screening underwent IP to extract the autoABs and their corresponding antigens. In the preclearing procedure, Protein G coupled magnetic beads, patients' sera, and mouse brain lysate (two technical replicates) were incubated together. Bound autoAB-antigen complexes were extracted and subsequently separated by SDS-PAGE. Replicate 1 was stained with Roti-Blue 5x to visualize protein bands. Replicate 2 was blotted onto a nitrocellulose membrane and incubated with its own serum to visualize the protein band that includes the target antigen structure. The target protein band identified on the membrane of replicate 2 was cut from the stained gel of replicate 1. (C) Every gel slice was prepared for MS, including destaining, alkylation, and trypsin digestion. Finally, all samples were compared with parallel prepared control samples. *Figure adapted from Van Beuningen et al., 2015.*

2.5 Validation of brain protein-reactive antibody binding in Western Blot

To confirm the presence of brain protein-reactive autoABs against potential neuronal targets in the index patient sample, a modified immunoblot method was used (Pitsch et al., 2020). Target proteins were either produced or purchased as a ready-to-use buffered solution. Discs large MAGUK scaffold protein 2 (DLG2) cDNA was cloned into a bacterial expression plasmid as a HIS-Tag (Polyhistidin) fusion protein to express the protein in BL21 (DE3) competent cells. Plakophilin 4 (PKP4) and Potassium voltage-gated channel subfamily C member 3 (KCNC3) cDNA were cloned into a mammalian expression plasmid as GFP (green fluorescent protein) Tag fusion proteins for expression in HEK293T cells. Porcine heart PDHc was purchased (Sigma-Aldrich, P7032-10U) and diluted with double-distilled H2O (0.625 mg/ml). All proteins were linearized by heating with 6x Laemmli buffer for 10 min at 95 °C and then loaded for SDS-PAGE (Laemmli, 1970). The gels were transferred onto nitrocellulose membranes, which were blocked afterwards, and washed as previously described. Proteins on the membranes were incubated with sera from seronegative patients suspected of AE, control sera and a commercial AB either murine monoclonal anti-PDHc AB cocktail (Abcam, ab110416, 1:1000), rabbit monoclonal anti-DLG2 (Abcam, ab151721, 1:1000), rabbit polyclonal anti-PKP4 (Abcam, ab2300855, 1:1000), or rabbit polyclonal anti-KCNC3 (ThermoFisher, PA5-41024). Binding patterns were visualized using secondary ABs including IRDye 800CW goat anti-human IgG (LI-COR Biosciences, 926-32232), goat anti-mouse IRDye 680DR (LI-COR Biosciences, 926-68070), and goat anti-rabbit IRDye 680RD (LI-COR Biosciences, 926-68071). Available CSF samples from patients were then screened in the same manner as described (dilution 1:1), with controls using CSF from seronegative patients suspected of AE without additional bands in the immunoblot screening.

2.6 Immunohistochemistry on wild-type mice paraffine sections

Adult wild-type mice (C57BL/6N) were sacrificed by decapitation under deep isoflurane anesthesia. The brains were then removed, fixed in paraformaldehyde (PFA), embedded in paraffin, and sectioned at 4 µm slices, which were subsequently allowed to air dry overnight at 37 °C. Sections were deparaffinized in a descending alcohol series. Endogenous peroxidase activity was blocked with 0.3 % H_2O_2 for 20 min at room temperature (RT), followed by antigen retrieval in 0.1 M citrate buffer (pH 6.0) using

microwave heating (600 W) for 2 cycles of 5 min each, according to standard protocol (Bauer and Lassmann, 2015). After washing in PBS, sections were incubated in 10 % normal goat serum (NGS) for 1 h at 37 °C to block non-specific binding sites. Sections were then incubated overnight at 4 °C with a commercially available murine monoclonal anti-PDHc AB cocktail (Abcam, ab110416, 1:200) together with either patients' anti-PDH AB-positive serum, serum from healthy controls or normal human serum (1:100). Following primary AB incubation, sections were treated with appropriate secondary ABs for 2 hours at RT (Alexa Fluor 488 goat anti-mouse AB (Life Technologies A-11001, 1:200), Alexa Fluor 568 goat anti-human AB (Thermo Fisher Scientific A-21090, 1:200), DAPI (2-Phenylindol) (Sigma-Aldrich D9542, 1:100.000) for nuclear staining) and mounted with Mowiol 4-88 (Roth, 713.2). Finally, the sections were imaged using a Nikon A1/T1 laser scanning confocal microscope.

2.7 Primary hippocampal neurons

Dissociated murine primary hippocampal neurons (PHNs) from embryonic day 15 to day 19 were prepared according previously established protocols (Van Loo et al., 2019) and cultured in NeuroBasal medium (Pitsch et al., 2020). Subsequently, some neurons were left untreated while others were virus transduced on day in vitro (DIV) 5 with either rAAV-mDlx (to label inhibitory neurons) or rAAV-vGLUT2 (to label excitatory neurons). All animal procedures were designed and performed to minimize pain and suffering, and to reduce the number of animals used in accordance with European, national, and institutional guidelines (guidelines of the European Parliament and of the Council on the protection of animals used for scientific purposes, European Directive (2010/63/EU), and the ARRIVE guidelines). The study protocol was approved by the Landesamt für Natur, Umweltschutz und Verbraucherschutz (LANUV) of the state of North Rhine Westphalia, Germany).

2.8 Immunocytochemistry on murine primary hippocampal neurons

On DIV 14 virus transduced or native PHNs were fixed in 4 % PFA for 10 min and then washed three times with PBS. Neurons were then permeabilized with 0.3 % Triton for 10 min and blocked in a solution containing 1 % BSA, 10 % NGS and 0.2 % Triton for 1 h at RT. After blocking, neurons were incubated overnight at 4 °C with appropriate primary ABs (mouse monoclonal anti-PDH complex AB cocktail (Abcam, ab110416, 1:1000); mouse anti-PDH E2 AB (Abcam, ab110332, 1:500); rabbit anti-PDH E2 AB (Abcam,

ab172617, 1:100); rabbit anti-PDH E1α AB (Sigma Aldrich, AP1064, dilution 1:500); rabbit anti-PDH E3 AB (Abcam, ab186827, 1:500)). After primary AB incubation, PHN were washed three times with PBS and then incubated with appropriate secondary ABs for one hour at RT (Alexa Fluor 488 goat anti-mouse AB (Life Technologies A-11001, 1:1000); Alexa Fluor 647 goat anti-mouse AB (Life Technologies A-21236, 1:1000); Alexa Fluor 568 goat anti-rabbit (Life Technologies A-11011, 1:1000); Alexa Fluor goat anti-guinea pig (Thermo Fisher Scientific A-11073, 1:1000), Alexa Fluor 568 goat anti-human AB (Thermo Fisher Scientific A-21090, 1:1000), together with DAPI (Sigma-Aldrich D9542, 1:100.000) for nuclear staining). After secondary AB incubation, PHNs were washed, mounted with Mowiol, and stored at 4 °C until imaging. Images were captured using a Nikon A1/T1 confocal microscope.

3. Results

3.1 KCNC3, DLG2, and PKP4 are not confirmed as autoantibody targets in seronegative patients suspected of having autoimmune encephalitis

To identify potential novel autoABs in seronegative patients suspected of having AE, we performed IP followed by MS of sera from 80 patients of our patient cohort who were tested positive in screening assays for non-specific brain protein-reactive autoABs (Fig. 5A, representative blot of one index patient) collected at the University Hospital Bonn (for details see 2.1 Patients). Samples selected for MS were chosen based on the presence of distinct protein bands on single SDS-PAGE gels that were not present in control samples. Notably, 9 sera showed strong additional bands that were not present in the controls (11%) (Fig. 5B, representative post-IP gel of one index patient). MS of these bands identified three abundant proteins related to neuronal plasticity that were not detected in any control sample based on protein abundances (for details see Tab. 1).

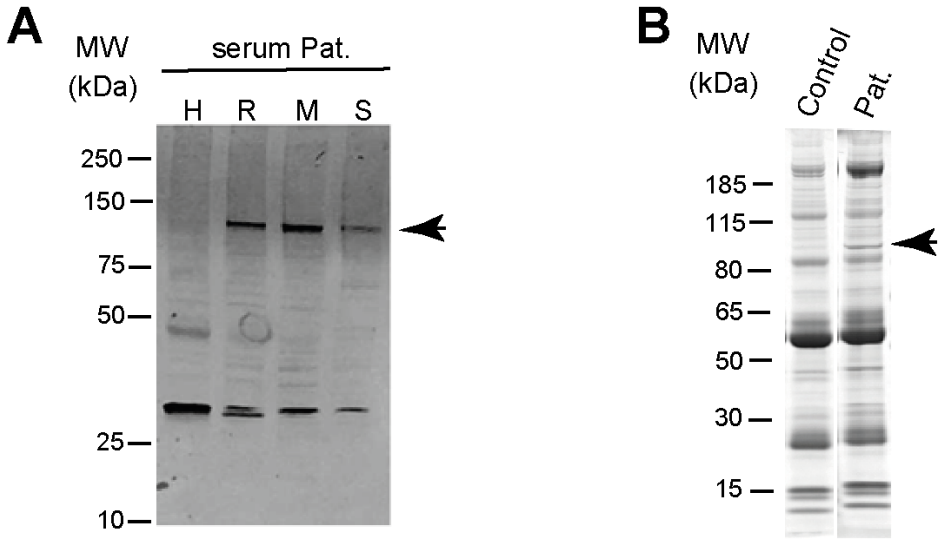

Fig. 5: Detection of additional band in SDS-PAGE gel after IP in seronegative, screening-positive patient serum. (A) Immunoblot from one seronegative patient incubated on human (H), rat (R), mouse (M), and mouse synaptosome (S) lysates reveals a distinct binding pattern (arrow). (B) Stained SDS-PAGE gel after IP with the same patient serum shows an additional band at the identical protein size observed in the immunoblot, which is sent for MS analysis (arrow).

Tab. 1: MS results with protein abundances of potential autoAB targets in index patients.

Protein ID	Name	Protein Symbol	MW [kDa]	Abundance (Index-Pat.)	Abundance (Ctrl.)	Ratio
Q63959	Potassium voltage-gated channel subfamily C member 3	KCNC3	82.1	1.9E+05	-	-
D3YUZ8	Disc large MAGUK scaffold protein 2	DLG2	83.9	5.2E+04	-	-
A2AS47	Plakophilin 4	PKP4	131.8	1.1E+05	-	-

The potential autoAB targets included

a) the Potassium voltage-gated channel subfamily C member 3 (KCNC3), a channel found in inhibitory GABAergic interneurons (Su et al., 2007),

b) the discs large MAGUK scaffold protein 2 (DLG2), a scaffold protein in excitatory synapses (Kim et al., 1996), and

c) Plakophilin 4 (PKP4), a protein involved in regulating intercellular adhesions (Keil et al., 2013).

To confirm the specificity of these proteins as autoAB targets, we performed immunoblot screening using index patient sera and purified protein of all three potential autoAB targets. However, the immunoblot of index patients' sera did not show any reactivity against purified KCNC3, DLG2, or PKP4 compared to commercial ABs (Fig. 6A-C). As none of these proteins were confirmed as autoAB target with our respective patients' sera by immunoblotting, we decided to revise and refine the method of identification.

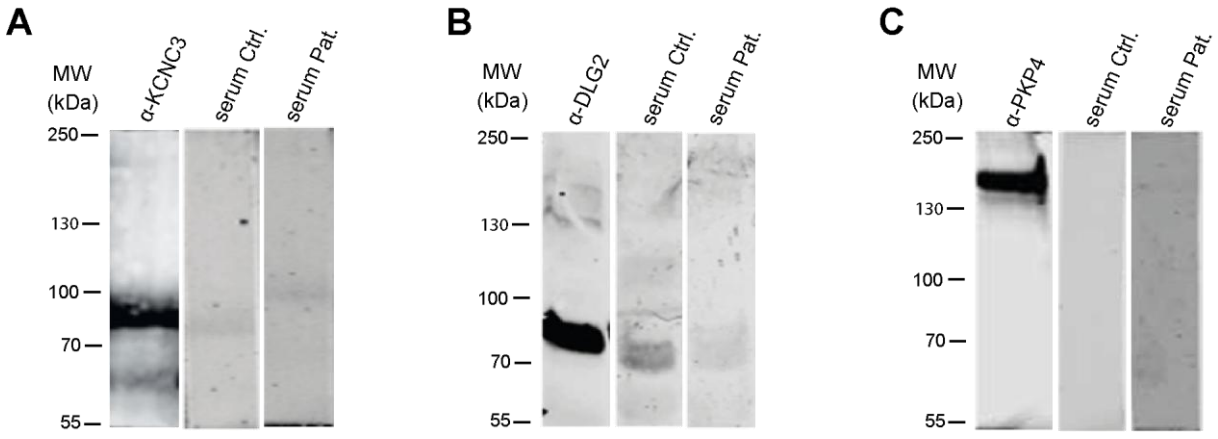

Fig. 6: AutoABs against KCNC3, DLG2, and PKP4 are not confirmed in our sera of patients with suspected AE. Immunoblots of purified (A) KCNC3, (B) DLG2, (C) PKP4 show no reactivity with serum of index patients and healthy control serum while commercial ABs revealed strong binding pattern at specific protein sizes.

3.2 Method optimization – Identification of potential neuronal autoantibody targets

As in our above described initial screening for potential targets of autoABs in sera of seronegative patients suspected of AE none of the proteins was confirmed in western blot screening, we wanted to optimize our method to increase reproducibility and develop a more widely applicable procedure. Therefore, the following modifications were made and validated in broad approaches. Parameters such as the preparation of the brain lysates, the type of lysis buffer, the definition of the control bands, the performance of further blots for verification and the improvement of the MS analysis were considered.

a) Preparation of brain lysate

Initially, brain lysates were cryopreserved for ease and flexibility in handling during IP procedures. However, to minimize potential protein denaturation caused by freezing and thawing, we tested freshly prepared mouse brain lysates. Additionally, we modified the centrifugation protocol by adding an ultracentrifugation step at 70.000 x g to obtain purer lysates according to protocols provided by Logopharm on their website in 2021 (Logopharm, 2021, accessed Jan 2021). Visual comparison of SDS-PAGE gels incubated with samples from the same patients using freshly prepared versus cryopreserved brain lysates with TX-100 detergent (Fig. 7A) showed that freshly prepared, ultracentrifuged brain lysate resulted in clearer, more distinct protein bands. For the following approaches, we used freshly prepared mouse brain lysate to achieve a higher accuracy in protein identification.

b) Type of lysis buffer

Given the unknown nature of the potential autoantigens, our aim was to find a buffer that can effectively solubilize a wide range of proteins. Due to a potential functional relevance of unidentified autoABs within the neuronal network, we focused particularly on synaptic plasma membrane proteins, such as receptors and associated proteins, but also intracellular synaptic proteins. Based on data from Logopharm on various solubilization buffers for neuronal proteins (Logopharm GmbH, 2017), we compared the results using the buffers CL 47 and CL 91 or our standard TX-100 buffer. IP was performed using negative control serum and serum suspected of containing putative brain protein-reactive autoABs under identical conditions for all three buffers. Visual inspection of the SDS-

PAGE gels (Fig. 7B) revealed that CL 47 provided the most distinct protein band differentiation, suggesting superior solubilization of neuronal proteins with minimal loss of protein structure, while TX-100 showed the poorest differentiation. For the following approaches, we used the CL 47 buffer in mouse brain lysate preparations to achieve a higher accuracy in protein identification.

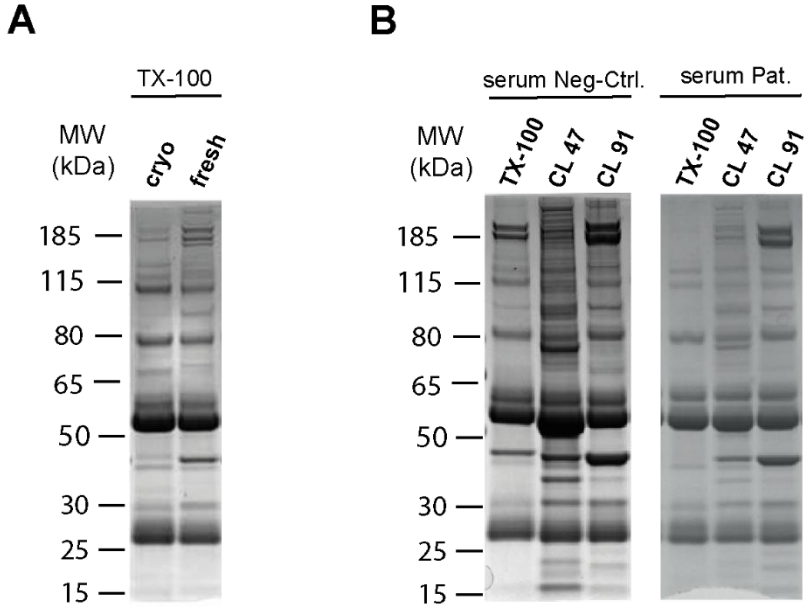

Fig. 7: Comparison of solubilization buffers and lysate preparation methods. Representative Coomassie-stained gels following IP and SDS-PAGE with mouse brain lysate. (A) Brain lysate was prepared using TX-100, either cryopreserved thawed, or freshly made with an additional ultracentrifugation step. A representative healthy control serum sample is shown, demonstrating that the freshly prepared and ultracentrifuged lysate resulted in clearer and more distinct protein bands compared to the cryopreserved lysate. (B) Fresh brain lysate was prepared using TX-100, CL 47, or CL 91 buffers. Representative serum samples from a healthy control and a suspected patient are shown, indicating that the lysate prepared with CL 47 achieved the most distinct protein band differentiation. Neg-Ctrl. – negative control. Cryo – cryopreserved. Fresh – freshly made. Pat. – patient. TX-100 –Triton X-100. CL 47 – ComplexioLyte 47 lysis buffer (Logopharm). CL 91 – ComplexioLyte 91 lysis buffer (Logopharm).

c) Definition of control bands

Initially, the control samples were handled according to Pitsch et al. (2020). The entire protein content of individual control samples was analyzed by halting SDS-PAGE early, before full protein separation recured, causing all proteins to accumulate in a single band. This method ensured that the entire protein content was sent for MS analysis in one band,

preventing the exclusion of any proteins. To improve the accuracy of our control analysis by preventing protein overloading, we performed SDS-PAGE on the six control samples in the same manner as for the patient samples, allowing complete protein separation within the gel. Each control lane was then divided into six bands, each containing a similar range of protein sizes: 185 -115 kDa, 115 -80 kDa, 80 -65 kDa, 65 -55 kDa, 55 -50 kDa, and 50 -30 kDa. In total, 36 control bands were sent for MS analysis (Fig. 8). We calculated the average protein abundance for each size range across the six control samples. This allowed a specific comparison between patient and control proteins. For instance, a patient band showing reactivity at ~85 kDa was compared only with the average MS results of the control bands within the 115 -80 kDa range. By implementing this approach with well-defined control bands, we achieved high accuracy in protein identification, which may lead to significant insights in distinguishing potential new autoantigens.

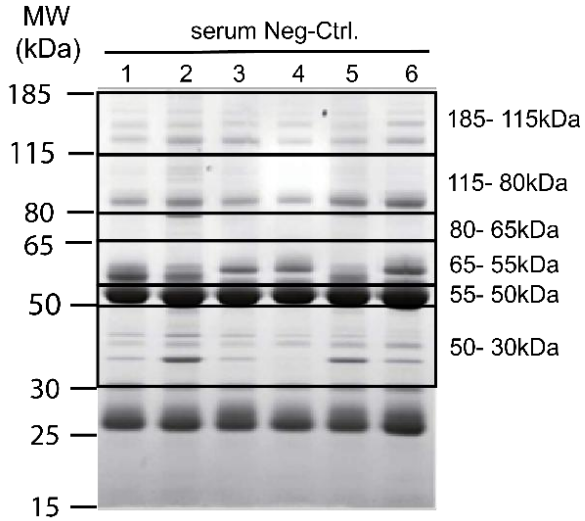

Fig. 8: Division of control samples into six fragments. Each gel lane of the control samples was divided into six specific ranges: 185 -115 kDa, 115 –80 kDa, 80 –65 kDa, 65 -55 kDa, 55 –50 kDa, and 50 –30 kDa, which were cut separately. All fragments were processed and sent for MS analysis.

d) Validation of protein bands in immunoblots

In our initial screening, 11 % of patient samples on stained SDS-PAGE gels met the visual standards (additional strong colored bands) for sending protein bands for MS analysis. We recognized that relying solely on these visual criteria could lead to overlooking of bands containing potential brain protein-reactive autoAB targets. As each band on SDS-

PAGE gels contains multiple proteins, a target antigen may be present but not visually detectable due to background protein interference. To address this, we added an additional confirmation step to improve the detection of putative antigens.

Two identical replicates of each serum sample were prepared using IP and SDS-PAGE as described above. One gel was stained as usual, while the other gel was blotted onto nitrocellulose membrane and incubated with the corresponding serum to visualize the protein band containing the potential autoAB target (for more details, see 2.4 IP and MS). To test this approach the additional confirmation step was performed using three sera of seronegative, screening-positive patients suspected of AE, three sera of healthy controls, and one anti-GAD65 autoAB positive sera. In the stained SDS-PAGE gel (replicate 1) of the anti-GAD65 autoAB positive biosample no additional protein bands were visible compared to seronegative healthy controls (Fig. 9A). However, the anti-GAD65 autoAB positive serum demonstrated a strong binding pattern at ~65 kDa in the post-IP immunoblot (replicate 2) (Fig. 9B). This protein band corresponds to the exact size of GAD65, indicating the binding of patient-derived anti-GAD65 autoABs with their target protein. The unremarkable staining of SDS-PAGE gel of anti-GAD65 autoAB positive biosample highlights the importance of not relying solely on visual criteria within stained gels to identify protein bands that contain potential brain protein-reactive autoAB targets, and rather making a validation of respective protein bands in immunoblots essential. All three sera of seronegative, screening-positive patients showed strong reactivity in post-IP immunoblots of protein bands (Fig. 9B) that were not striking in the corresponding stained SDS-PAGE gels (Fig. 9A). Based on these findings, we implemented the immunoblot confirmation step for the following procedures. By modifying this approach, we improved the accuracy of identifying proteins bands with potential brain protein-reactive autoABs, reducing the chance of missing significant antigens in so far seronegative AE patients.

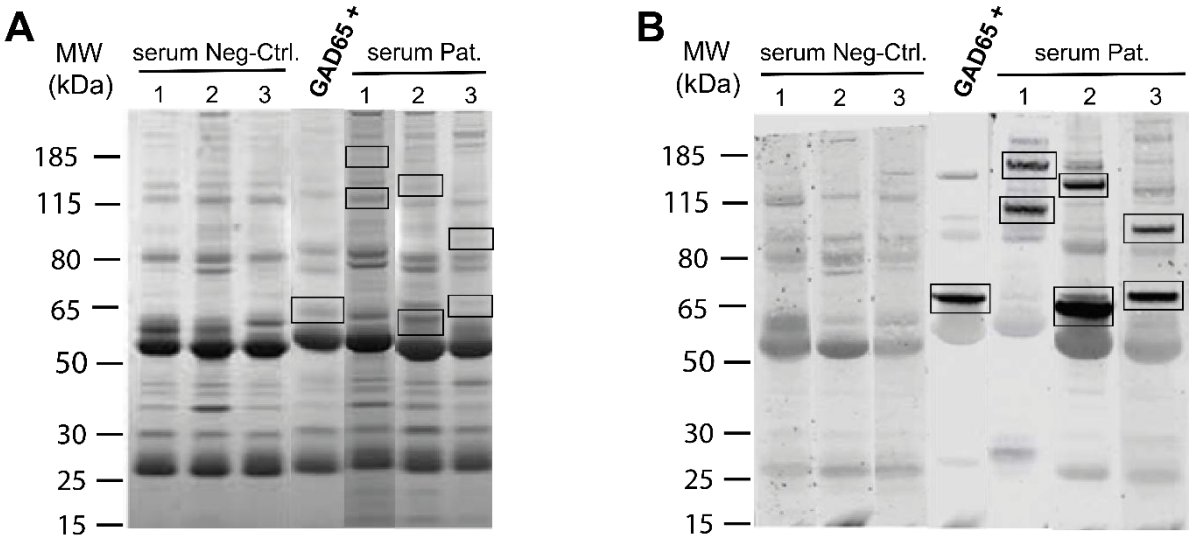

Fig. 9: Identification of protein bands containing brain protein-reactive autoAB targets in immunoblot. (A) Roti-Blue 5x-stained gel and corresponding (B) immunoblot after IP and separation with SDS-PAGE. Neg-Ctrl. – negative control sera. Pat. – seronegative screening-positive sera. GAD65+ – anti-GAD65 autoAB positive serum.

e) MS analysis of autoantibody targets

To identify potential autoABs targets within the protein bands cut from SDS-PAGE gels, MS analysis was performed with data evaluation by comparing protein abundances in patients' samples to control samples.

In our initial analysis, three proteins of interest (KCNC3, DLG2, and PKP4) were detected in MS. Their protein abundances were relatively low (up to xE+05), while no corresponding abundances were detected in control samples (for details see Tab. 1). However, immunoblot confirmation failed to validate these proteins as autoAB targets in index patients' sera, suggesting that the measured abundances might fall below the threshold for meaningful detection.

To refine the analysis, MS was performed using a positive control biosample with anti-GAD65 autoABs. This revealed a significantly higher GAD65 abundance (3E+10) compared to controls (3E+03), resulting in a GAD65/Ctrl ratio of 9.9E+06. In contrast, proteins commonly identified as non-specific in MS showed a lower average protein abundance (up to ~ 2E+07), with a much lower protein/Ctrl ratio (up to ~ 2E+01).

Based on these findings, we established new thresholds for MS data analysis to improve the specificity of autoAB target identification:

1. Protein abundance ≥ 2E+07.
2. Sample/Ctrl ratio ≥ 2E+01.

These revised criteria refined the MS analysis, enhancing the ability to identify meaningful antigens while minimizing false positives results.

In summary, by improving the sensitivity and specificity of our method for detecting potentially relevant brain protein-reactive patient-derived autoABs, we tested several modifications. The use of freshly prepared, ultracentrifuged brain lysates, the CL 47 buffer, the definition of the control bands, the inclusion of immunoblot visualization and the adjustment of the MS protein cut-off resulted in more precise results.

3.3. PDH complex as autoantibody target structure in patients suspected of autoimmune encephalitis

3.3.1 Identification of PDH complex as antigen of brain protein-reactive autoantibodies

To identify potential targets of brain protein-reactive autoABs in seronegative, but screening-positive sera of patients suspected of AE in order to reveal an underlying connection within this patient group, the newly introduced protocol described above was now implemented. Therefore, 55 patient sera samples of our cohort of patients suspected of AE at the University Hospital Bonn that were screened negative for known neuronal but strongly positive for unspecific brain protein-reactive autoABs (for details see 2.1. Patients) were processed with IP followed by MS. Seventeen samples (31 %) that were highly reactive on Western blots (Fig. 10A-B, representative blot Pat. #1) and post-IP immunoblots (Fig. 10C, representative blot Pat. #1) were sent for MS analysis. Using the adjusted cut-offs for protein abundance, not only the E2 and E3 subunits of the PDHc were identified in three patients (Pat. #1 - #3), but also the E1 subunit in two patients (Pat. #1 - #2) (for details see Tab. 2).

To confirm the presence of autoABs against the three different PDHc subunits in samples of all three index patients, a protein-specific immunoblot was performed using commercial porcine heart PDHc protein. As expected, serum of Pat. #1 and #2 showed strong

reactivity according to the subunits E2, E3, and E1α, whereas Pat. #3 exhibited a binding pattern only with E2 and E3 subunit (Fig. 10D). Respective available CSF samples from Pat. #1 and Pat. #2 revealed similar binding patterns to the corresponding serum samples (Fig. 10E). For Pat. #3 no CSF sample was available.

Tab. 2: MS results with the protein abundances of PDHc in index patients #1 -#3. Green – protein abundance above threshold for potential autoAB target; white – protein abundance below threshold for potential autoAB target.

Protein ID	Name	Protein Symbol	PDH subunit	MW [kDa]	Abundance (Pat.)	Abundance (Ctrl.)	Ratio
		Pat.#1					
Q8BMF4	Dihydrolipoyllysine-residue acetyltransferase	DLAT	E2	67.9	9.2E+09	1.6E+07	5.6E+02
Q8BKZ9	Dihydrolipoamide dehydrogenase	DLD	E3	54	4.5E+07	7.8E+05	5.8E+01
P35486	Pyruvate dehydrogenase E1 component subunit alpha	PDHa1	E1α	43.2	3.3E+10	6.7E+06	4.9E+03
		Pat.#2					
Q8BMF4	Dihydrolipoyllysine-residue acetyltransferase	DLAT	E2	67.9	7.1E+09	3.7E+07	1.9E+02
Q8BKZ9	Dihydrolipoamide dehydrogenase	DLD	E3	54	8.6E+07	7.8E+05	1.1E+02
P35486	Pyruvate dehydrogenase E1 component subunit alpha	PDHa1	E1α	43.2	4.6E+10	6.7E+06	6.8E+03
		Pat.#3					
Q8BMF4	Dihydrolipoyllysine-residue acetyltransferase	DLAT	E2	67.9	4.4E+10	1.6E+07	2.7E+03
Q8BKZ9	Dihydrolipoamide dehydrogenase	DLD	E3	54	9.4E+07	1.9E+05	4.8E+02
P35486	Pyruvate dehydrogenase E1 component subunit alpha	PDHa1	E1α	43.2	1.7E+07	8.4E+06	2.0E+00

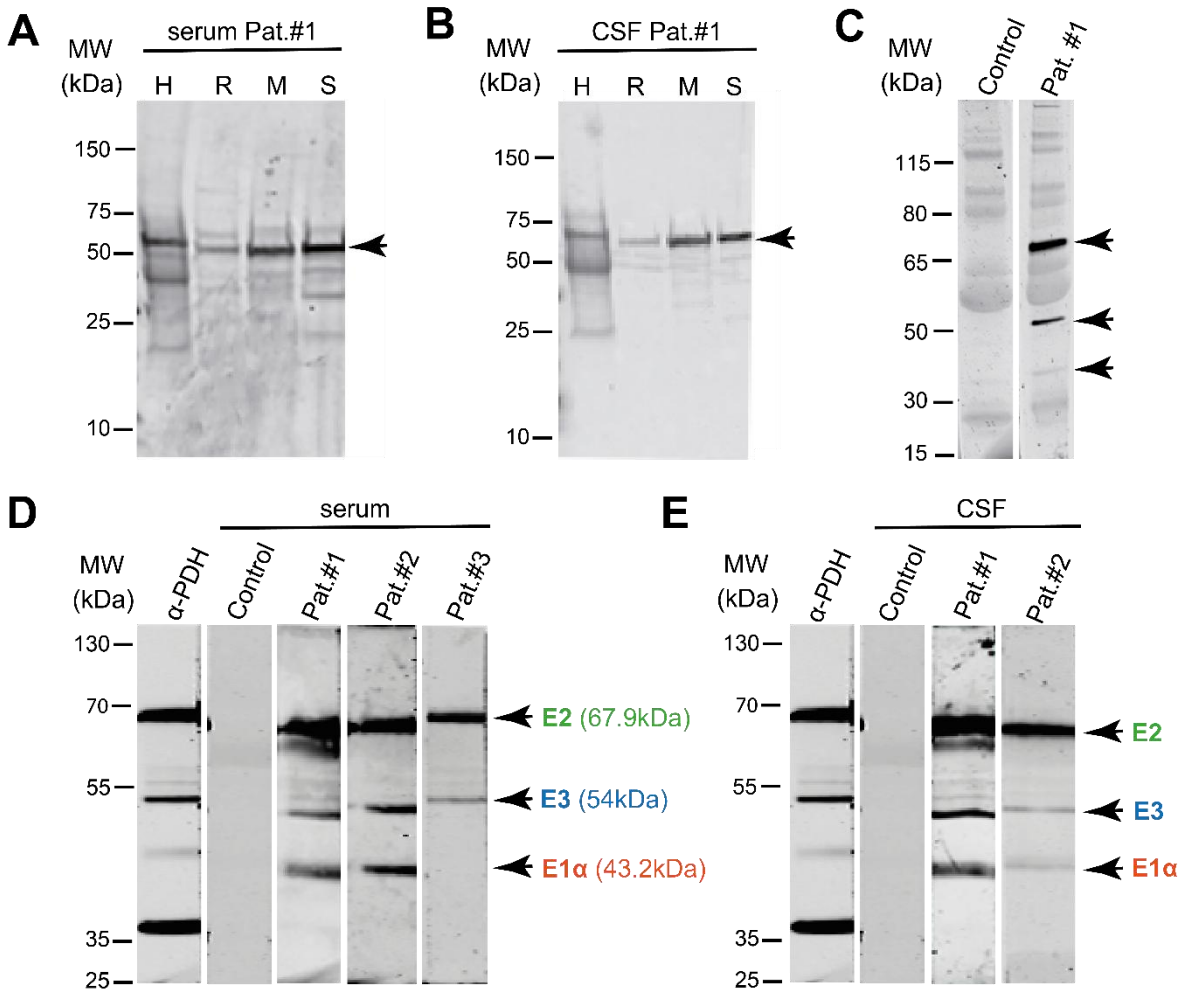

Fig. 10: PDHc subunits were identified as target antigens of autoABs in serum samples of seronegative patients suspected of AE. Representative western blot of (A) serum and (B) CSF samples of the index patient #1 (Pat. #1) incubated on brain lysate of human (H), rat (R), mouse (M) and mouse synaptosome (S) revealed a remarkable strong binding pattern (arrows). (C) Representative immunoblot after IP performed with serum of Pat. #1 showing bands (arrows) identified by MS as different subunits of PDHc (E2, E3, E1α) compared to a healthy control sample. (D) In immunoblots performed with PDHc protein sera of all three index patients showed reactivity against E2, E3, E1α (Pat. #1, Pat. #2) or E2 and E3 (Pat. #3) (arrows). (E) CSF of Pat. #1 and Pat. #2 showed reactivity against the same subunits identified by corresponding sera (arrows).

3.3.2 E2 subunit of the PDH complex as main epitope for autoantibodies

To assess the prevalence of anti-PDH autoABs in seronegative patients suspected of AE, a further 332 of these patients who showed strong additional bands < 110 kDa in the initial brain protein-specific immunoblot screening were validated. Of these, a further nine

patients (Pat. #4 - #12) were screened positive for anti-PDHc autoABs using serum samples (Fig. 11).

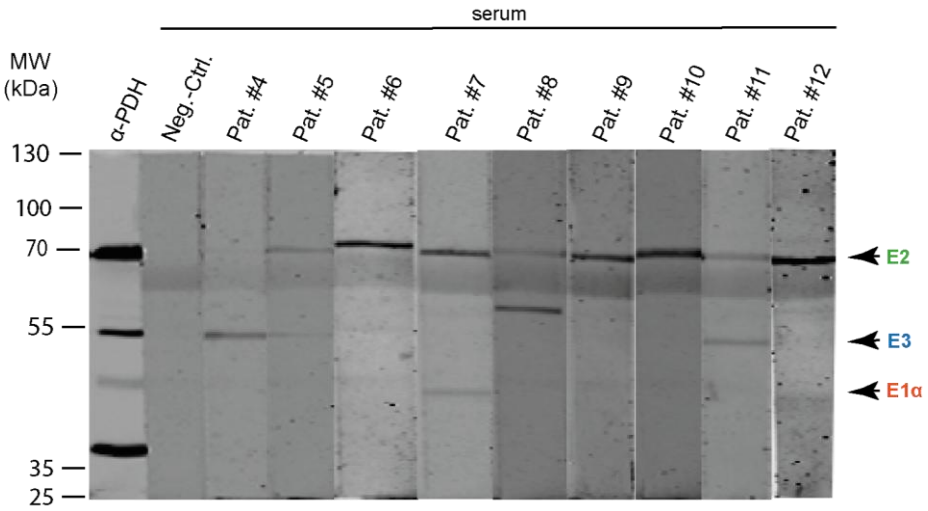

Fig. 11: Identification of 9 previously seronegative patients' sera being positive for autoABs against different subunits (E2, E3, E1α) of the PDHc in immunoblot screening.

Out of the 12 positive patients, 11 patients were positive for anti-E2 autoABs (92%). Four patients were positive for only one of the three autoABs against PDHc subunits, while eight patients presented with a combination of two or three different autoABs (Fig. 10D-E and Fig. 11) (for details see Tab. 3).

To quantify the amount of autoABs in positive patients, serum and CSF samples were titrated. The titer of anti-PDHc autoABs ranged from 1:100 up to 1:250,000 in sera and from 1:1 up to 1:10,000 in CSF.

Tab. 3: Distribution of autoABs against different subunits of the PDHc in patients positive for anti-PDHc autoABs.

		autoAB details					
		1 autoAB			2 autoABs		3 autoABs
subunits		E1α	E2	E3	E1α| E2	E2| E3	E1α| E2| E3
number of patients	12	0	3	1	1	4	3
			4		5		3

		autoAB total		
subunits		E1α	E2	E3
number of patients	12	4	11	8

3.3.3 Clinical analysis of anti-PDH complex autoantibody positive patients

Out of all 12 anti-PDHc positive patients (n(male) =6, n(female) =6; median age 50, 25% percentile 30.5, 75% percentile 55), 10 patients presented with epileptic seizures including focal and/or generalized seizures (for details see Tab. 4). Focal to bilateral tonic-clonic seizures were the most frequent seizure type observed (n =6). Two patients experienced seizure-like episodes, transient loss of consciousness, or amnesia. Upon reviewing cMRI images, nine out of 12 patients showed abnormalities. Four patients displayed hyperintensity on T2-weighted FLAIR sequences in the temporal lobe (hippocampus and/or amygdala), either unilateral or bilateral. The remaining five patients exhibited hyperintensity in multifocal areas, including both white and grey matter. CSF analysis revealed increased protein levels in at least three patients and mononuclear cell pleocytosis in at least two patients. These findings can indicate disruption of BBB, intrathecal synthesis of autoABs, or general intracerebral inflammation. In addition to seizures, nine out of 10 examined patients exhibited significant neuropsychological alterations, including deficits in short-term, verbal, and/or figural memory, altered mental status, and cognitive impairments. Notably, five patients presented with psychiatric symptoms. These psychiatric symptoms ranged from bipolar disorder to depression and post-traumatic stress disorder. Three patients had previously been diagnosed with other autoimmune diseases, such as PBC, psoriasis, or Hashimoto`s thyroiditis. Nine patients were treated with single or combination of ASMs following commonly approved guidelines, tailored to individual side effects. Three patients did not receive any anti-seizure therapy. None of the patients received immunosuppressive therapy, and none underwent epileptic surgery. During the follow-up one patient achieved seizure freedom. Eleven patients had ongoing seizures under ASM. Two patients of these became pharmacoresistant defined as seizures unresponsive to at least two ASMs, while the other nine patients did not meet the criteria for pharmacoresistant epilepsy. Data on outcomes and treatment of non-seizure symptoms were unavailable.

Tab. 4: Clinical characteristics and demographic features of anti-PDHc positive patients.

Characteristics	anti-PDH associated patients
Number of patients	n =12
Sex (m/ f)	n =6/ n =6
Age of onset (median, years)	50 (25% percentile: 30.5/ 75% percentile: 55, min 17/ max 79)
CSF analysis (✓/ x/)	n =10/ n =2
Protein ↑	n =3
Pleocytosis	n =2
no abnormalities	n =5
available for autoAB screening	n =3
cMRI (✓/ x/)	n =12/ n =0
Hyperintensity temporal lobe unilateral	n =2
Hyperintensity temporal lobe bilateral	n =2
Hyperintensity white matter	n =4
Hyperintensity grey matter	n =1
no abnormalities	n =3
Seizures (✓/ x/)	n =10/ n =2
focal + bilateral tonic-clonic	n =6
bilateral tonic-clonic	n =4
other*	n =2
Neuropsychologic examination (✓/ x/)	n =10/ n =2
altered**	n =9
no abnormalities	n =1
Psychiatric Symptoms (✓/ x/)	n =5/ n =7
Bipolar disorder	n =1
Depression	n =3
Post-traumatic stress disorder	n =1
Comorbid autoimmune diseases (✓/ x/)	n =3/ n =9
Primary biliary cholangitis	n =1
Psoriasis	n =1
Hashimoto thyroiditis	n =1
Malignant diseases (✓/ x/)	n =0/ n =12
Therapy	
ASM	n =9
Immunosuppressive therapy	n =0
Epilepsy surgery	n =0
No seizure treatment	n =3
Outcome	
Seizure freedom	n =1
Ongoing seizures	n =9
Pharmacoresistant***	n =2

✓ – yes, x - no

* dropouts, loss of conscioiusness, amnesia

** deficits in short-term, verbal and figural memory, altered mental status

*** seizure unresponsive to at least two ASMs

3.4 PDH complex as neuronal autoantibody target in seronegative patients suspected of autoimmune encephalitis

3.4.1 PDH complex expression in cerebellum, cerebral cortex, and hippocampal formation

To investigate the distribution of PDHc in various brain regions murine wildtype brain slices were stained with a commercial anti-PDHc AB. To confirm the presence of anti-PDHc autoABs in patients' sera and to investigate the binding pattern of patients-derived anti-PDHc autoABs the murine wildtype brain slices were furthermore stained with suspected patients' sera. On the one hand the commercial AB demonstrated a strong binding pattern in granular cells of cerebellum (Fig. 12A, small square top), in the cerebral cortex (Fig. 12A, small square bottom), and in the hippocampal formation, with the strongest labeling observed in the CA3 region (Fig. 12B), therefore identifying the PDHc as a widespread constitute of the CNS. On the other hand, the suspected patients' sera (Fig. 12, representative immunostaining of serum Pat. #3) exhibited a strong colocalization with the commercial AB across all those three brain regions. This confirmed the presence of anti-PDHc autoABs in the sera of the novel identified patient cohort with suspected AE and furthermore revealed an identical binding pattern with the commercial AB.

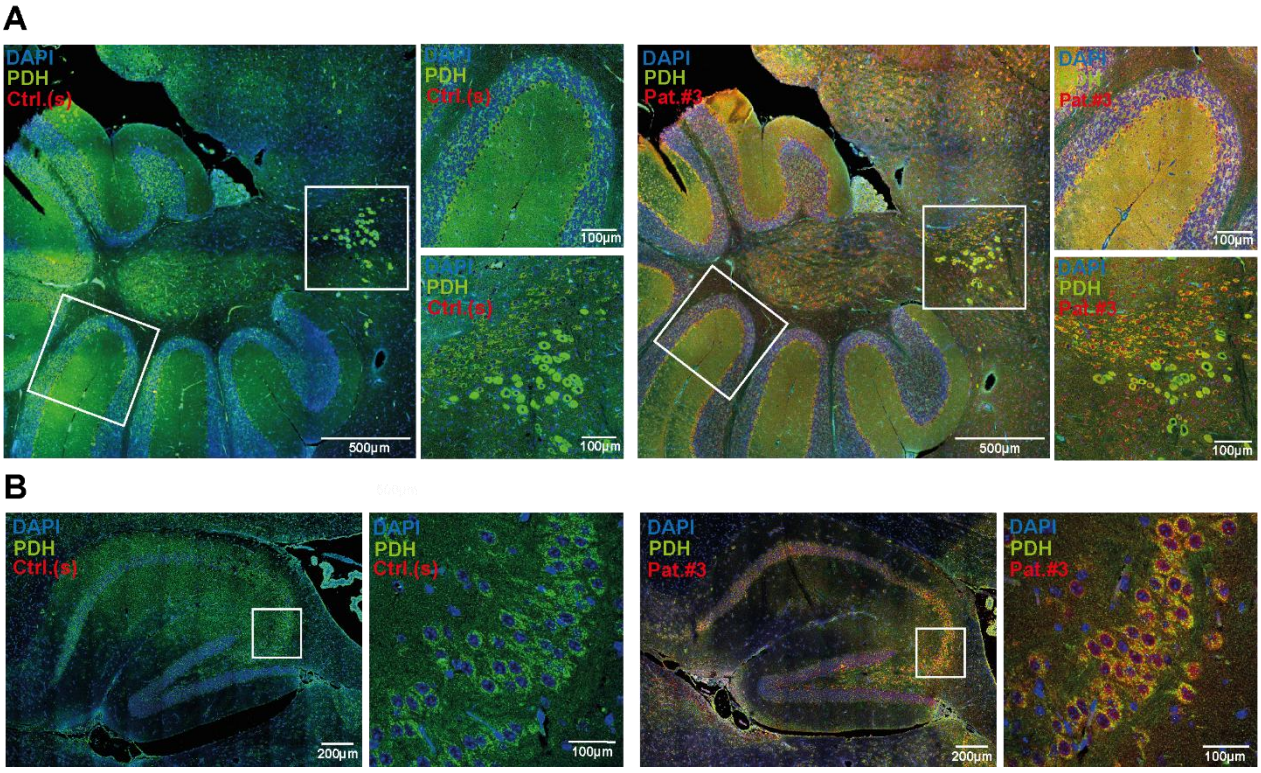

Fig. 12: PDHc expression in murine wildtype brain slices. Immunostaining of mouse brain slices using commercial anti-PDHc AB and anti-PDHc autoAB positive patient serum reveals strong colocalization in different brain regions. (A) Serum from Pat. #3 and mouse monoclonal anti-PDHc AB cocktail exhibit strong colocalization in granular cells of the cerebellum (top square) and cerebral cortex (bottom square) of mouse brain slices. In contrast, no reactivity is observed with serum from seronegative human controls. (B) Serum from Pat. #3 and mouse monoclonal anti-PDHc AB cocktail show strong colocalization within the hippocampal formation of mouse brain slices, particularly in the CA3 region, which is absent in controls.

3.4.2 PDH complex expression in inhibitory and exhibitory neurons

To explore the localization of the PDHc within neurons and to investigate the binding pattern of patient-derived anti-PDHc autoABs on neuronal structures, we conducted experiments using PHNs. First, we used commercial monoclonal ABs against the subunits E2, E3 and E1α together with a mouse monoclonal anti-PDHc AB cocktail that contains ABs against the different subunits to assess colocalization among these subunits within PHNs (Fig. 13). Our findings revealed strong colocalization among the ABs targeting each subunit, indicating the integration of these subunits into a large PDHc and confirming the presence of the complete complex within neuronal tissue.

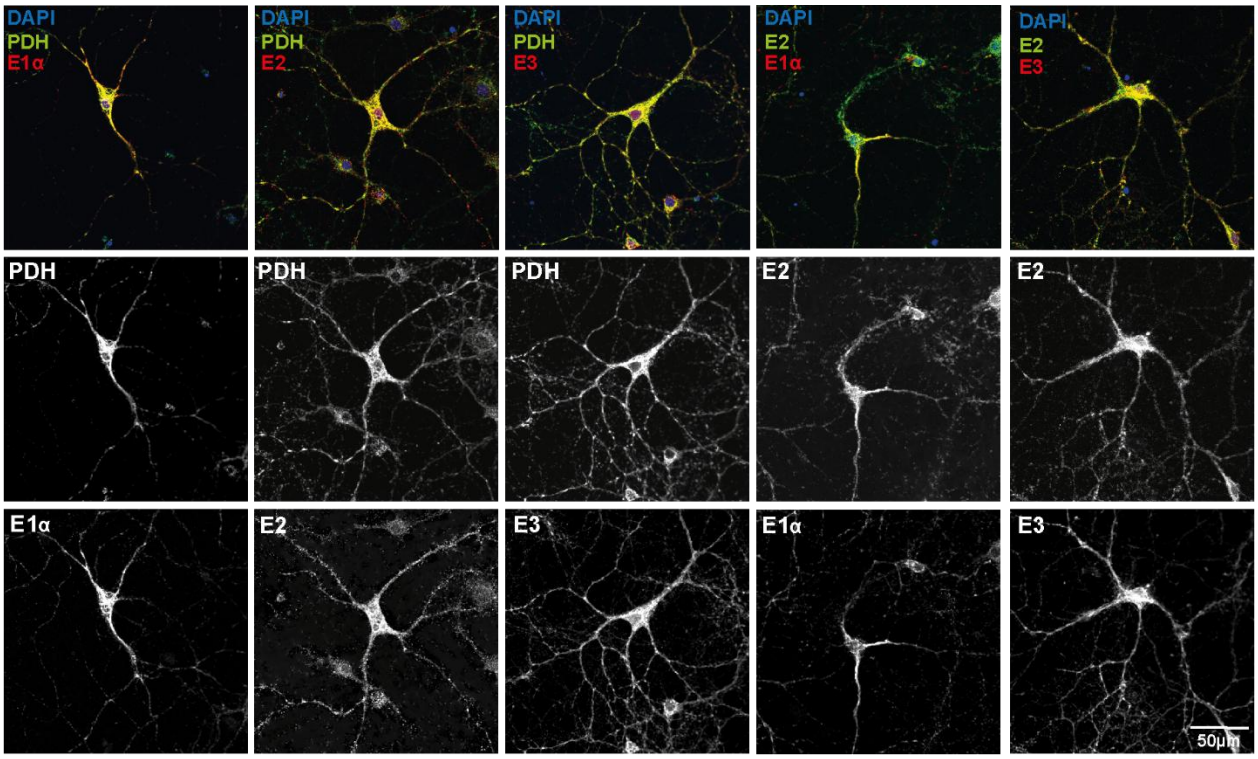

Fig. 13: Immunostainings of PHNs with mouse monoclonal ABs against different subunits of the PDHc (E1α, E2, E3) and mouse monoclonal anti-PDHc AB cocktail show strong colocalization among each other.

Following incubation of PHNs with commercial anti-PDHc AB, healthy human sera, and anti-PDHc positive patients' sera, patients' sera revealed strong colocalization with commercial anti-PDHc AB indicating an identical binding pattern on neuronal dendrites and soma (Fig. 14, right, representative immunostainings of serum Pat. #1 - #3) while healthy human sera revealed no reactivity (Fig. 14, left).

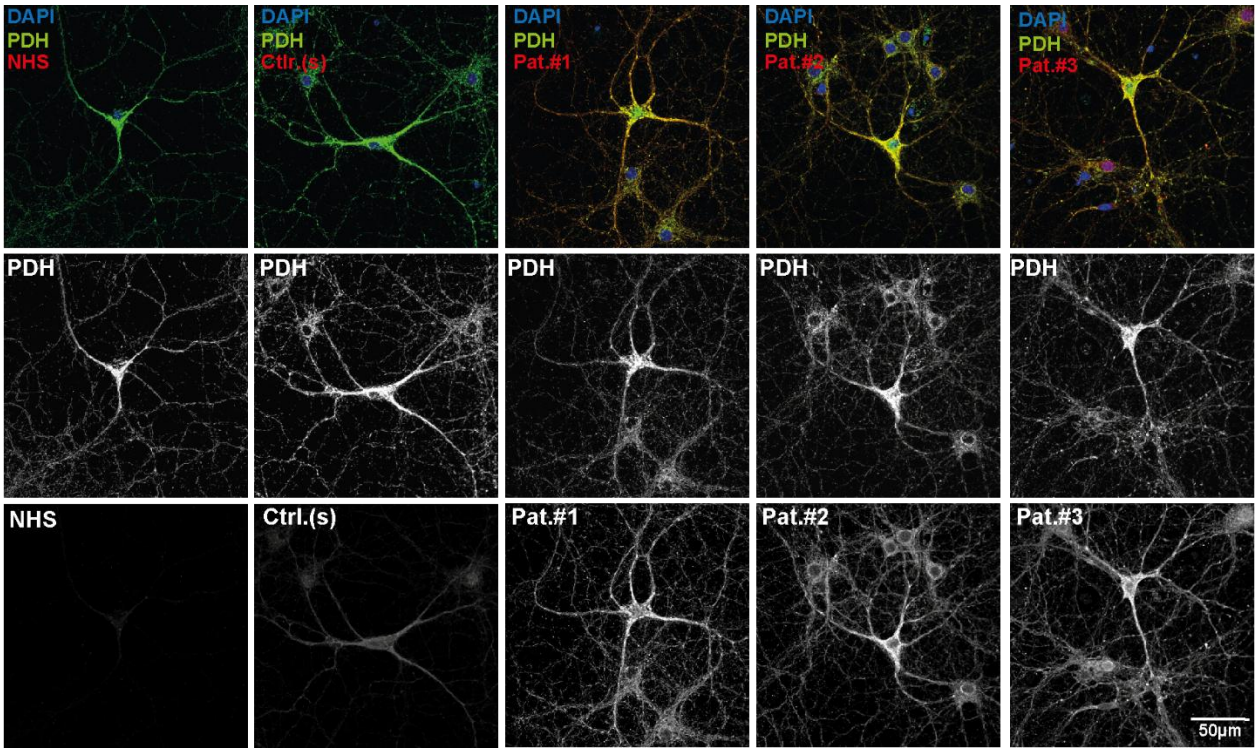

Fig. 14: Immunostainings of PHNs with mouse monoclonal anti-PDHc AB and anti-PDHc positive patients' sera (index patients #1 - #3) strongly label neuronal dendrites and soma. No colocalization is observed with serum from seronegative healthy control.

Furthermore, commercial anti-PDHc AB showed strong reactivity on dendritic spines (Fig. 15, middle) while anti-PDHc positive patients' sera revealed strong colocalization (Fig. 15, bottom, right) which was notably absent in control sera (Fig. 15, bottom, left).

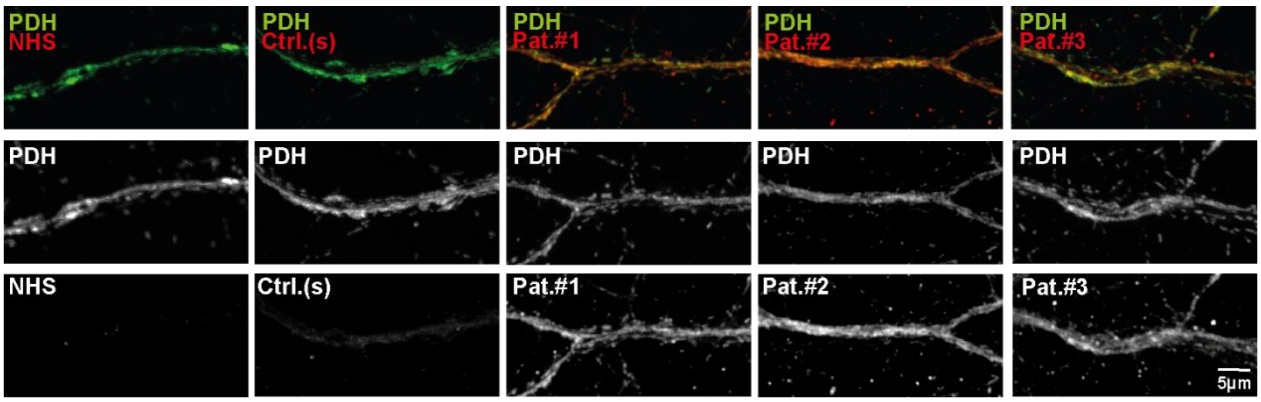

Fig. 15: Immunostaining of PHNs with mouse monoclonal anti-PDHc AB and anti-PDHc positive patients' sera (index patients #1 - #3) strongly label dendritic spines. No colocalization is observed with serum from seronegative healthy control.

To further explore the presence of PDHc in inhibitory interneurons (transduced with rAAV-mDlx, blue; Fig. 16A, right) and excitatory neurons (transduced with rAAV-Glut2, pink; Fig. 16B, right), PNHs were incubated with commercial anti-PDHc ABs, anti-PDH positive patients' serum, and human control serum. We observed a strong binding pattern of commercial anti-PDHc AB on both inhibitory (Fig. 16A, middle) and excitatory neurons (Fig. 16B, middle) with strong co-immunolabeling of anti-PDHc positive patients' sera (Fig. 16A-B, bottom, representative immunostaining of serum Pat. #1), which was absent in controls (Fig. 16A-B, top). Remarkably, the signals were stronger on inhibitory dendrites than on exhibitory dendrites, indicating a higher density of the PDHc in inhibitory neurons.

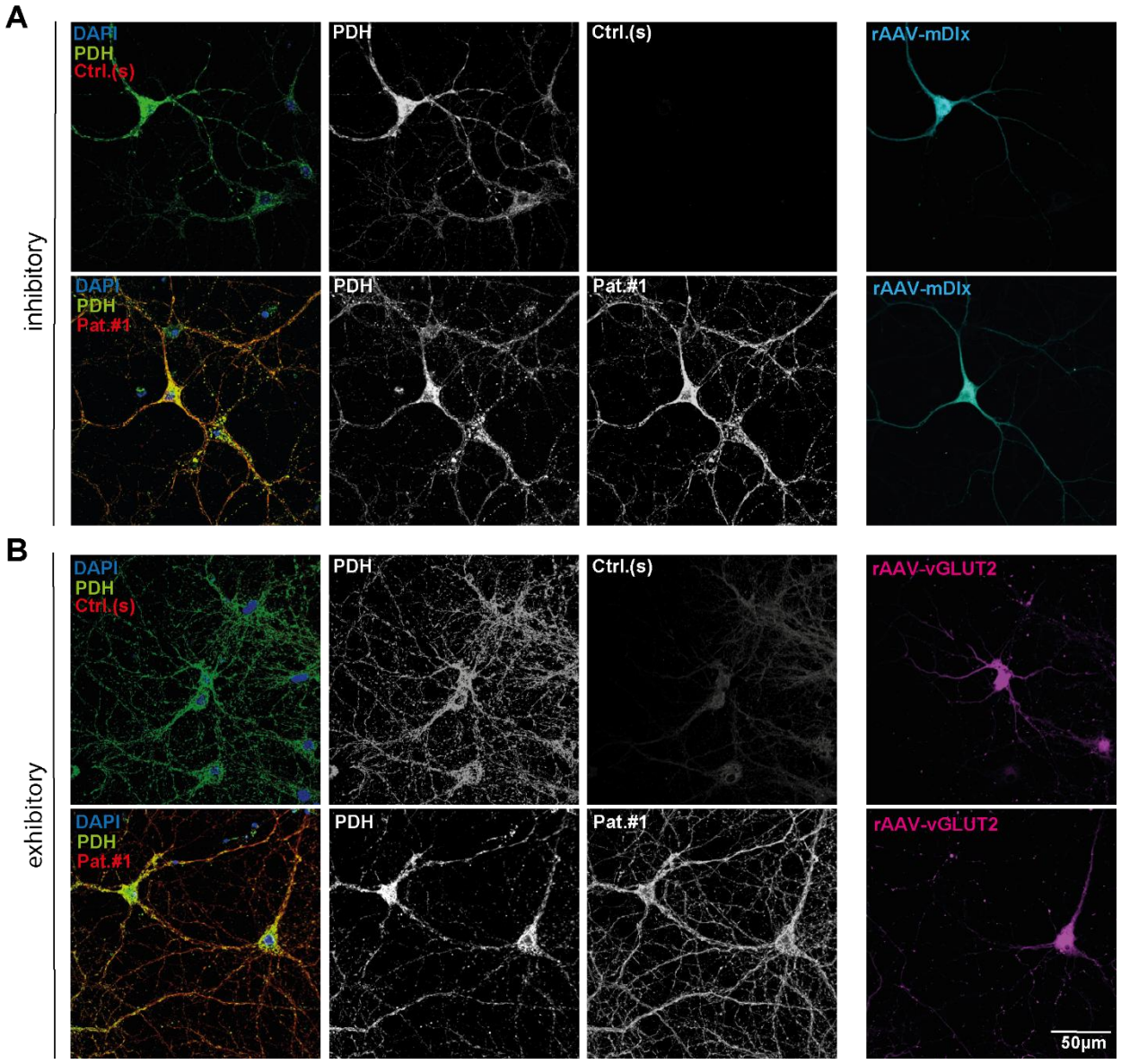

Fig. 16: Immunostaining of inhibitory and excitatory neurons with anti-PDHc positive serum and commercial anti-PDHc AB. (A) Anti-PDHc autoAB positive serum (Pat. #1) demonstrates strong colocalization with commercial mouse monoclonal anti-PDHc AB on rAAV-mDlx transduced inhibitory interneurons. Control seronegative human serum shows no binding pattern in inhibitory hippocampal neurons. (B) Anti-PDHc autoAB positive serum (Pat.#1) exhibited colocalization with commercial mouse monoclonal anti-PDHc AB on rAAV-Glut2 transduced excitatory hippocampal neurons. Control seronegative human serum shows no colocalization.

4. Discussion

The main aim of this thesis was to analyze seronegative biosamples of patients with clinical suspicion of having AE who have been tested negative for known AE- associated autoABs but who were tested positive in screenings for brain protein- reactive ABs. We wanted to assess a possible underlying connection within this patient group by focusing on potential so far unidentified brain protein- reactive autoABs.

A critical aim was to refine the process of identifying putative antigens in brain tissue. Compared to previous works e.g. by Pitsch et al. (2020) we could successfully optimize our protocol by introducing several key modifications that significantly enhanced the detection of brain protein- reactive autoAB targets. Pitsch et al. (2020) employed brain lysate preparations without ultracentrifugation and by using TX-100 as detergent instead of freshly made lysate with a buffer (CL47) that provided more optimal conditions for neuronal protein stability. Among other modifications, the integration of a validation step by using immunoblot visualization of potential protein bands alongside the adjustment of the MS protein abundance cuff-off was a key step in increasing the sensitivity, specificity, and reproducibility of the previously published method to identify potential novel antigens (Pitsch et al., 2020).

By implementing this approach, we were able to identify autoABs against the intramitochondrial PDHc in sera within our cohort of seronegative patients suspected of AE at the University Hospital Bonn. So far, known associated autoABs in AE can target different structures within the CNS, either neuronal surface proteins or intracellular antigens (Dalmau and Graus, 2018; Geis et al., 2019). While autoABs targeting surface antigens seem to have a direct pathogenic effect leading to abnormal neuronal activity, intracellular or intraorganellar autoABs are rather believed serving as biomarkers while the brain immunopathology is mainly mediated by cytotoxic T cells (Bien et al., 2012; Zhang et al., 2013). The PDHc, located within the inner MM (Stacpoole and McCall, 2023), is theoretically less accessible by autoABs as their uptake would require passage through two membrane barriers. Given this challenge, the presence of anti-PDHc autoABs may function primarily as a novel biomarker in AE, similar to AE- associated autoABs that target functionally irrelevant intranuclear proteins such as HU, Ma2/Ta or YO (Graus et al.,

2010). This consideration would suggest their role as more indicative of disease processes rather than directly contributing to pathology.

However, recent discoveries have identified a new intracellular targeting autoAB with direct pathophysiological consequences. Notably, anti-Drebrin autoABs were detected in patients with previously seronegative AE. To our best knowledge, anti-Drebrin represents the first autoAB associated with AE that targets an intracellular protein, demonstrating cellular autoAB uptake with direct pathological effects in cell-based assays (Pitsch et al., 2020). Drebrin is a structural protein in postsynapses of excitatory neurons that plays a crucial role in actin cytoskeleton dynamics and synaptic function, making it a functionally relevant target for autoABs (Ferhat, 2012; Pitsch et al., 2020).

The intramitochondrial PDHc represents the key link between glycolysis and the citric acid cycle and is therefore crucial for the aerobic energy system, ensuring sufficient oxygen availability. Among all organ systems, the CNS has the highest oxygen demand, making it particularly vulnerable to ischemia and hypoxia, which can lead to neuronal dysfunction and cell death (Angamo et al., 2016; Liu et al., 2021). As the primary source of ATP, mitochondria are highly abundant in neuronal tissue and exhibit dynamic intracellular movement, allowing to meet varying energy demand across different neuronal compartments (Matsumoto et al., 2022; Safiulina and Kaasik, 2013; Zsurka and Kunz, 2015). In addition to ATP production, mitochondria play a key role in neurotransmitter synthesis, calcium homoeostasis, and reactive oxygen species (ROS) regulation. Consequently, mitochondrial dysfunction has been implicated as primary factor in epileptogenesis (Davis and Williams, 2012; Zsurka and Kunz, 2015). Genetic mutations affecting oxidative decarboxylation or mitochondrial oxidative phosphorylation can result in epilepsy syndromes, as seen in patients with PDCD, who frequently present with developmental delay, epilepsy, and cerebral atrophy (Ganetzky et al., 2021).

Beyond genetic causes, acquired mitochondrial dysfunction has also been associated with epilepsy, including HS (Folbergrová and Kunz, 2012). Notably, mitochondrial dysfunction has been observed predominantly in the CA3 and CA4 regions of the hippocampus (Kunz et al., 2000). In our immunohistochemical analyses of murine brain slices, PDHc expression was detected throughout the brain, with notably higher density in the CA3 region of the hippocampal formation. Given the hippocampus known vulnerability

in AE (Bauer and Bien, 2016) and the role of mitochondrial dysfunction in seizure generation (Zsurka and Kunz, 2015), the PDHc as representative of a mitochondrial-rich structure within the CA3 region, may serve as a relevant target in the pathogenesis of AE. Anti-PDHc autoABs could contribute to neurologic deficits in AE through direct inhibition of oxidative decarboxylation within mitochondria. Additionally, secondary mitochondrial impairment could arise as consequence of higher energy demands during seizure activity, further promoting seizure generation (Kann et al., 2011; Kann and Kovács, 2007). Such metabolic stress may lead to increased exposure of the PDHc to the immune system, potentially driving secondary autoAB formation as already known for several intracellular autoABs in AE (Bien et al., 2012).

Mitochondrial oxidative phosphorylation failure has been implicated in seizure generation through multiple mechanistic pathways (Zsurka and Kunz, 2015). Studies on neuronal energy metabolisms have demonstrated that a significant proportion of presynaptic ATP is required for mobilizing synaptic vesicles containing neurotransmitters (Rangaraju et al., 2014). Consequently, inhibitory interneurons are particularly susceptible to energy deficits, as mitochondrial dysfunction can lead to a decreased synaptic transmission and contribute directly to increased network excitability (Kann et al., 2011; Kann and Kovács, 2007). In our immunocytochemical analysis of PHNs, PDHc expression was detected in both inhibitory and excitatory neurons, with a notably stronger signal on inhibitory dendrites. This finding suggests a higher mitochondria density in inhibitory interneurons, supporting the hypothesis that these cells rely on oxidative phosphorylation and are therefore especially vulnerable to mitochondrial dysfunction (Gulyás et al., 2006), Given the role of inhibitory interneurons in maintaining network stability, their selective impairment could contribute to the pathophysiology of AE, further highlighting the PDHc as potential relevant target protein in AE.

Beyond its role in seizure generation, mitochondrial dysfunction has also been implicated in the pathophysiology of various neuropsychiatric disorders. Recent studies have identified structural and functional abnormalities in the mitochondria of post-mortem brain samples from patients with schizophrenia (Roberts, 2017). Additionally, genetic analyses have revealed an association between schizophrenia and nuclear-encoded mitochondrial variants, further supporting mitochondrial dysfunction as a potential underlying

mechanism in this disorder (Nakagami et al., 2020,; Schulmann et al., 2019). Notably, anti-PDH E1α autoABs have recently been detected in a small subgroup of patients with schizophrenia, suggesting a possible autoimmune component contributing to the pathogenesis of this disease (Nakagami et al., 2020).

Given the broad spectrum of clinical presentations in AE patients, the symptomatic inclusion criteria in our patient cohort were diverse (Leypoldt et al., 2013). Nevertheless, in our clinical analysis of anti-PDHc autoAB positive AE patients, psychiatric symptoms were observed in almost half of cases, alongside seizures, although no direct comparison with a healthy control cohort was conducted. Considering recent insights into the pathological background of schizophrenia, a link between mitochondrial dysfunction, potentially PDHc impairments, and psychiatric symptoms in both schizophrenia and anti-PDHc positive patients suspected of AE represents a discovery that requires further investigations.

When considering anti-PDHc autoABs it becomes clear that they belong to the broader group of AMAs, which are strongly associated with PBC. Among these, autoABs targeting the M2 antigen are a particularly sensitive marker for PBC (Colapietro et al., 2022; Kumagi and Heathcote, 2008). Notably, only one patient in our cohort had a previously known diagnosis of PBC. However, given that PBC can remain asymptomatic for years, and our inclusion criteria did not screen for hepatic or cholestatic dysfunction (Kumagi und Heathcote, 2008), it remains possible that subclinical or undiagnosed cases were present. Furthermore, as longitudinal data were not available, future development of overt hepatic manifestations cannot be ruled out.

Traditionally, anti-PDHc autoABs have been considered a biomarker of PBC. However, emerging evidence suggests a more active role in pathogenesis (Chen et al., 2022). In PBC, immune dysregulation involves both innate and adaptive pathways with immune responses targeting biliary epithelial cells (Gulamhusein and Hirschfield, 2018). AMAs, including those against the PDHc, can stimulate proinflammatory cytokine release via interactions with macrophages and apoptotic blebs, that retain intact E2 antigens (Chen et al., 2022; Gulamhusein and Hirschfield, 2018). This immune cascade facilitates both, the production of autoABs and the activation of autoreactive T cells directed against epithelial tissue (Shimoda et al., 2006; Shimoda et al., 1998). Our data did not deal with

the pathogenic potential of the anti-PDHc autoABs but they identified three different subunits of the PDHc as targets for autoAB recognition (E2, E3, E1α) in anti-PDHc positive patients suspected of AE. This pattern mirrors the autoAB profiles observed in PBC, where approximately 95% of patients reveal autoABs against the E2 subunit (Colapietro et al., 2022). Although no clear link between subunit specificity and clinical presentation has been established in PBC, E2 is considered the immunodominant epitope due to its lipoyl domain, which can initiate and amplify immune responses. This may promote epitope spreading to neighboring domains or subunits and contribute to cross-reactivity within the PDHc (Backes et al., 2011; Gulamhusein and Hirschfield, 2018; Rigopoulou and Bogdanos, 2023; Yang et al., 2022). While our cohort is not powered to assess a potential clinical impact of subunit-specific autoABs in anti-PDHc autoAB associated AE, the recognition of multiple PDHc subunits raises the possibility of a shared immunopathologic mechanism between PBC and anti-PDHc positive AE. In this context, anti-PDHc autoABs may contribute to CNS-specific autoimmunity through mechanism analogous to those described in hepatic tissue, involving antigen-presenting cells and damaged neuronal structures. These findings underscore the need for further investigation into the pathogenic role of AMAs beyond the liver and their broader relevance in autoimmune diseases as is becomes clear that those autoABs can also be detected in other autoimmune diseases such as Sjögren’s syndrome, SLE, APS, or inflammatory myositis (Colapietro et al., 2022; Favoino et al., 2023; Pisetsky et al., 2020).

Autoimmune diseases frequently overlap, with patients often developing multiple immune-mediated conditions (Kumagi and Heathcote, 2008). This phenomenon is also seen in AE, where patients may present with additional autoimmune comorbidities, suggesting a broader dysregulation of immune tolerance across organ systems (McKeon and Tracy, 2017). In our cohort of anti-PDHc autoAB positive patients suspected of AE one third had a previously diagnosed autoimmune disease, including psoriasis, Hashimoto’s thyroiditis and PBC potentially suggesting a broader systemic immune dysregulation that extends beyond individual organ systems. Although we did not specifically assess the possible relationship between pre-existing autoimmune disease and neurologic manifestation, the link between peripheral autoimmunity and CNS involvement becomes an area of growing interest. In neuropsychiatric systemic lupus erythematosus (NPSLE) both the central and

peripheral tissues can be targeted. Seizures and neuropsychiatric symptoms may precede systemic signs and are driven by autoABs, proinflammatory cytokines, and autoreactive T cells targeting neuronal and endothelial structures, contributing to BBB disruption that triggers neuroinflammation (Andrade et al., 2008; Justiz-Vaillant et al., 2024). Although the concept of peripheral autoimmunity contributing to neuroinflammation and seizure activity is subject of current studies, the relationship between peripheral autoimmune response and AE particularly in patients with anti-PDHc autoABs requires further investigation.

The identification of anti-PDHc autoABs in patients suspected of AE reinforces the growing evidence of mitochondrial dysfunction as a potential contributor to neurological disorders. Given the established role of AMAs in various autoimmune conditions, the presence of anti-PDHc autoABs may signal a broader immune dysregulation linking central and peripheral autoimmune processes. The co-occurrence of other autoimmune conditions in affected patients supports that immune responses may not be organ-specific but reflect systemic immune dysregulation. Further research is needed to clarify the pathogenic significance of anti-PDHc autoABs in AE and to explore their potential implications for diagnosis and treatment strategies.

5. Summary

The aim of this thesis was to analyze biosamples of seronegative patients suspicious of autoimmune encephalitis (AE) who were screened positively in a brain protein-reactive immunoblot by focusing on detecting potential so far unidentified brain protein-specific autoantibodies (autoABs).

In the first step, we optimized the method for identifying brain protein-reactive autoABs by improving critical steps, including an immunoblot confirmation step to verify additional bands.

Next, we analyzed biosamples from 387 patients who presented to the University Hospital Bonn, Germany, between 2017 and 2021 with clinical symptoms of AE but without known autoABs to identify potential brain protein-reactive autoABs in serum or cerebrospinal fluid. Mass spectrometry identified three subunits of the intramitochondrial pyruvate dehydrogenase complex (PDHc) as target proteins in serum samples of three different index patients, including pyruvate dehydrogenase E1 component subunit α (E1α), dihydrolipoyllysine-residue acetyltransferase (E2), and dihydrolipoamide dehydrogenase (E3). Subsequently, we identified a total of 12 patients positive for anti-PDHc autoABs through immunoblotting in our cohort, with E2 being the major autoABs target.

In a third step we conducted an initial characterization of the identified autoABs and their targets, by using immunohistochemistry on murine brain slices and immunocytochemistry on primary hippocampal neurons. Localization studies revealed that the PDHc is widely distributed in the cerebral cortex, cerebellum, and hippocampus, as well as at dendritic spines and soma of mainly inhibitory but also excitatory neurons.

Anti-PDHc autoABs are present in previously seronegative patients with suspected AE and may play a role in this disease spectrum. However, the potential pathological relevance of the autoABs themselves, associated mitochondrial dysfunction, the involved immunologic reactions, and an in-depth clinical implication regarding disease onset, course, and prognosis require further investigation.

6. List of Figures

7. List of Tables

8. References

Andrade RM, Alarcón GS, González LA, Fernández M, Apte M, Vilá LM, McGwin G, Reveille JD. Seizures in patients with systemic lupus erythematosus: data from LUMINA, a multiethnic cohort (LUMINA LIV). Ann. Rheum. Dis. Ann Rheum Dis, 2008; 67: 829–834

Andrejevic S, Bonaci-Nikolic B, Sefik-Bukilica M, Petrovic R. Clinical and serological follow-up of 71 patients with anti-mitochondrial type 5 antibodies. Lupus. Lupus, 2007; 16: 788–793

Angamo EA, Rösner J, Liotta A, Kovács R, Heinemann U. A neuronal lactate uptake inhibitor slows recovery of extracellular ion concentration changes in the hippocampal CA3 region by affecting energy metabolism. J. Neurophysiol. J Neurophysiol, 2016; 116: 2420–2430

Backes C, Ludwig N, Leidinger P, Harz C, Hoffmann J, Keller A, Meese E, Lenhof HP. Immunogenicity of autoantigens. BMC Genomics. BMC Genomics, 2011; 12

Bataller L, Rosenfeld MR, Graus F, Vilchez JJ, Cheung NK V., Dalmau J. Autoantigen diversity in the opsoclonus-myoclonus syndrome. Ann. Neurol. Ann Neurol, 2003; 53: 347–353

Bauer J, Bien CG. Neuropathology of autoimmune encephalitides. Autoimmune Neurol. 2016; 133: 107–120

Bauer J, Lassmann H. Neuropathological techniques to investigate central nervous system sections in multiple sclerosis. Methods Mol. Biol. Humana Press Inc., 2015; 1304: 211–229

Berg JM, Tymoczko JL, Gatto GJ, Stryer L. Biochemie. Berlin: Springer Spektrum, 2020

Berg PA, Klein R. Antimitochondrial antibodies in primary biliary cirrhosis and other disorders: definition and clinical relevance. Dig. Dis. Dig Dis, 1992; 10: 85–101

Berg PA, Ph D, Klein R. Heterogeneity of Antimitochondrial Antibodies. 1989;

Van Beuningen SFB, Will L, Harterink M, Chazeau A, Van Battum EY, Frias CP, et al. TRIM46 Controls Neuronal Polarity and Axon Specification by Driving the Formation of Parallel Microtubule Arrays. Neuron. Cell Press, 2015; 88: 1208–1226

Bien CG. Limbic encephalitis. Handb. Clin. Neurol. Elsevier B.V., 2022; 187: 467–487

Bien CG, Scheffer IE. Autoantibodies and epilepsy. Epilepsia. Epilepsia, 2011; 52 Suppl 3: 18–22

Bien CG, Urbach H, Schramm J, Soeder BM, Becker AJ, Voltz R, Vincent A, Elger CE. Limbic encephalitis as a precipitating event in adult-onset temporal lobe epilepsy. Neurology. Neurology, 2007; 69: 1236–1244

Bien CG, Vincent A, Barnett MH, Becker AJ, Blümcke I, Graus F, Jellinger KA, Reuss DE, Ribalta T, Schlegel J, Sutton I, Lassmann H, Bauer J. Immunopathology of autoantibody-associated encephalitides: Clues for pathogenesis. Brain. Oxford University Press, 2012; 135: 1622–1638

Brechet A, Buchert R, Schwenk J, Boudkkazi S, Zolles G, Siquier-Pernet K, et al. AMPA-receptor specific biogenesis complexes control synaptic transmission and intellectual ability. Nat. Commun. 2017; 8

Brenner T, Sills GJ, Hart Y, Howell S, Waters P, Brodie MJ, Vincent A, Lang B. Prevalence of neurologic autoantibodies in cohorts of patients with new and established epilepsy. Epilepsia. Epilepsia, 2013; 54: 1028–1035

Chen R, Tang R, Gershwin ME. Immunologic Responses and the Pathophysiology of Primary Biliary Cholangitis. 2022; 26: 583–611

Ciszak EM, Makal A, Hong YS, Vettaikkorumakankauv AK, Korotchkina LG, Patel MS. How Dihydrolipoamide Dehydrogenase-binding Protein Binds Dihydrolipoamide Dehydrogenase in the Human Pyruvate Dehydrogenase Complex. J. Biol. Chem. Elsevier, 2006; 281: 648–655

Colapietro F, Lleo A, Generali E. Antimitochondrial Antibodies: from Bench to Bedside. Clin. Rev. Allergy Immunol. Springer US, 2022; 63: 166–177

Dalmau J, Graus F. Antibody-Mediated Encephalitis. N. Engl. J. Med. New England Journal of Medicine (NEJM/MMS), 2018; 378: 840–851

Dalmau J, Rosenfeld MR. Paraneoplastic syndromes of the CNS. Lancet. Neurol. Lancet Neurol, 2008; 7: 327–340

Dalmau J, Tüzün E, Wu HY, Masjuan J, Rossi JE, Voloschin A, Baehring JM, Shimazaki H, Koide R, King D, Mason W, Sansing LH, Dichter MA, Rosenfeld MR, Lynch DR. Paraneoplastic anti-N-methyl-D-aspartate receptor encephalitis associated with ovarian teratoma. Ann. Neurol. Ann Neurol, 2007; 61: 25–36

Darnell RB, Posner JB. Paraneoplastic syndromes involving the nervous system. N. Engl. J. Med. N Engl J Med, 2003; 349: 1543–1554

Davis PA, Leung P, Manns M, Kaplan M, Munoz SJ, Gorin FA, Dickson ER, Krawitt E, Coppel R, Gershwin ME. M4 and M9 antibodies in the overlap syndrome of primary biliary cirrhosis and chronic active hepatitis: epitopes or epiphenomena? Hepatoloy, 1992; 16: 1128-1136

Davis RE, Williams M. Mitochondrial function and dysfunction: an update. J. Pharmacol. Exp. Ther. J Pharmacol Exp Ther, 2012; 342: 598–607

Favoino E, Grapsi E, Barbuti G, Liakouli V, Ruscitti P, Foti C, Giacomelli R, Perosa F. Systemic sclerosis and primary biliary cholangitis share an antibody population with identical specificity. Clin. Exp. Immunol. Clin Exp Immunol, 2023; 212: 32–38

Ferhat L. Potential role of drebrin a, an f-actin binding protein, in reactive synaptic plasticity after pilocarpine-induced seizures: functional implications in epilepsy. Int. J. Cell Biol. Int J Cell Biol, 2012; 2012

Folbergrová J, Kunz WS. Mitochondrial dysfunction in epilepsy. Mitochondrion. Mitochondrion, 2012; 12: 35–40

Ganetzky R, McCormick EM, Falk MJ. Primary Pyruvate Dehydrogenase Complex Deficiency Overview. GeneReviews®. University of Washington, Seattle, 2021;

Geis C, Planagumà J, Carreño M, Graus F, Dalmau J. Autoimmune seizures and epilepsy. J. Clin. Invest. 2019; 129: 926–940

Gleichman AJ, Spruce LA, Dalmau J, Seeholzer SH, Lynch DR. Anti-NMDA receptor encephalitis antibody binding is dependent on amino acid identity of a small region within the GluN1 amino terminal domain. J. Neurosci. J Neurosci, 2012; 32: 11082–11094

Gole S, Anand A. Autoimmune Encephalitis. StatPearls. 2025;

Graus F, Saiz A, Dalmau J. Antibodies and neuronal autoimmune disorders of the CNS. J. Neurol. J Neurol, 2010; 257: 509–517

Graus F, Titulaer MJ, Balu R, Benseler S, Bien CG, Cellucci T, et al. A clinical approach to diagnosis of autoimmune encephalitis. Lancet Neurol. Lancet Neurol, 2016; 4:391-404

Grob PJ, Häcki MA, Müller-Schoop JW, Joller-Jemelka HI. Drug-induced pseudolupus. Lancet (London, England). Lancet, 1975; 2: 144–148

Gulamhusein AF, Hirschfield GM. Pathophysiology of primary biliary cholangitis. Best Pract. Res. Clin. Gastroenterol. Bailliere Tindall Ltd, 2018; 34–35: 17–25

Gulyás AI, Buzsáki G, Freund TF, Hirase H. Populations of hippocampal inhibitory neurons express different levels of cytochrome c. Eur. J. Neurosci. Eur J Neurosci, 2006; 23: 2581–2594

Heine J, Prüss H, Bartsch T, Ploner CJ, Paul F, Finke C. Imaging of autoimmune encephalitis--Relevance for clinical practice and hippocampal function. Neuroscience. Neuroscience, 2015; 309: 68–83

Houri I, Hirschfield GM. Primary Biliary Cholangitis: Pathophysiology. Clin. Liver Dis. W.B. Saunders, 2024; 28: 79–92

Jarius S, Wandinger KP, Horn S, Heuer H, Wildemann B. A new Purkinje cell antibody (anti-Ca) associated with subacute cerebellar ataxia: Immunological characterization. J. Neuroinflammation. 2010; 7: 1–19

Joshi S, Cauch-Dudek K, Heathcote EJ, Lindor K, Jorgensen R, Klein R. Antimitochondrial antibody profiles: Are they valid prognostic indicators in primary biliary cirrhosis? Am. J. Gastroenterol. 2002; 97: 999–1002

Justiz-Vaillant AA, Gopaul D, Soodeen S, Arozarena-Fundora R, Barbosa OA, Unakal C, Thompson R, Pandit B, Umakanthan S, Akpaka PE. Neuropsychiatric Systemic Lupus Erythematosus: Molecules Involved in Its Imunopathogenesis, Clinical Features, and Treatment. Molecules. Molecules, 2024; 29

Kann O, Huchzermeyer C, Kovács R, Wirtz S, Schuelke M. Gamma oscillations in the hippocampus require high complex I gene expression and strong functional performance of mitochondria. Brain. Brain, 2011; 134: 345–358

Kann O, Kovács R. Mitochondria and neuronal activity. Am. J. Physiol. Cell Physiol. Am J Physiol Cell Physiol, 2007; 292

Kao YC, Lin MI, Weng WC, Lee WT. Neuropsychiatric Disorders Due to Limbic Encephalitis: Immunologic Aspect. Int. J. Mol. Sci. Multidisciplinary Digital Publishing Institute (MDPI), 2021; 22: 1–21

Keil R, Schulz J, Hatzfeld M. p0071/PKP4, a multifunctional protein coordinating cell adhesion with cytoskeletal organization. Biol. Chem. Biol Chem, 2013; 394: 1005–1017

Kim E, Cho KO, Rothschild A, Sheng M. Heteromultimerization and NMDA receptor-clustering activity of Chapsyn- 110, a member of the PSD-95 family of proteins. Neuron. Cell Press, 1996; 17: 103–113

Kuehn JC, Meschede C, Helmstaedter C, Surges R, von Wrede R, Hattingen E, Vatter H, Elger CE, Schoch S, Becker AJ, Pitsch J. Adult-onset temporal lobe epilepsy suspicious for autoimmune pathogenesis: Autoantibody prevalence and clinical correlates. PLoS One. 2020; 15: 1–18

Kumagi T, Heathcote EJ. Primary biliary cirrhosis. Orphanet J. Rare Dis. 2008; 3

Kunz WS, Kudin AP, Vielhaber S, Blümcke I, Zuschratter W, Schramm J, Beck H, Elger CE. Mitochondrial complex I deficiency in the epileptic focus of patients with temporal lobe

epilepsy. Ann. Neurol. John Wiley & Sons, Ltd, 2000; 48: 766–773

Laemmli UK. Cleavage of structural proteins during the assembly of the head of bacteriophage T4. Nature. Nature, 1970; 227: 680–685

Lai M, Hughes EG, Peng X, Zhou L, Gleichman AJ, Shu H, Matá S, Kremens D, Vitaliani R, Geschwind MD, Bataller L, Kalb RG, Davis R, Graus F, Lynch DR, Dalmau J, Balice-Gordon R. AMPA receptor antibodies in limbic encephalitis alter synaptic receptor location. Ann. Neurol. Ann Neurol, 2009; 65: 424–434

Lai M, Huijbers MGM, Lancaster E, Graus F, Bataller L, Balice-Gordon R, Cowell JK, Dalmau J. Investigation of LGI1 as the antigen in limbic encephalitis previously attributed to potassium channels: A case series. Lancet Neurol. Lancet Publishing Group, 2010; 9: 776–785

Lancaster E, Huijbers MGM, Bar V, Boronat A, Wong A, Martinez-Hernandez E, Wilson C, Jacobs D, Lai M, Walker RW, Graus F, Bataller L, Illa I, Markx S, Strauss KA, Peles E, Scherer SS, Dalmau J. Investigations of caspr2, an autoantigen of encephalitis and neuromyotonia. Ann. Neurol. Ann Neurol, 2011; 69: 303–311

Lancaster E, Lai M, Peng X, Hughes E, Constantinescu R, Raizer J, Friedman D, Skeen MB, Grisold W, Kimura A, Ohta K, Iizuka T, Guzman M, Graus F, Moss SJ, Balice-Gordon R, Dalmau J. Antibodies to the GABA(B) receptor in limbic encephalitis with seizures: case series and characterisation of the antigen. Lancet. Neurol. Lancet Neurol, 2010; 9: 67–76

Leung PSC, Coppel RL, Ansari A, Munoz S, Gershwin ME. Antimitochondrial antibodies in primary biliary cirrhosis. Semin. Liver Dis. Semin Liver Dis, 1997; 17: 61–69

Leypoldt F, Wandinger KP, Bien CG, Dalmau J. Autoimmune encephalitis. Eur. Neurol. Rev. Touch Briefings, 2013; 8: 31–37

Liu J, Gu Y, Guo M, Ji X. Neuroprotective effects and mechanisms of ischemic/hypoxic preconditioning on neurological diseases. CNS Neurosci. Ther. CNS Neurosci Ther, 2021; 27: 869–882

Logopharm GmbH. Description Complexiolytes 2017. Tuebingen: internal documentation,

rev02.11.2017. Unpublished document, received in 2021

Logopharm. Instructions for the use of Complexiolyte Buffers. 2021. https://www.logopharm.com/products-and-services/complexiolyte-buffers, accessed Jan 2021.

Van Loo KMJ, Rummel CK, Pitsch J, Müller JA, Bikbaev AF, Martinez-Chavez E, Blaess S, Dietrich D, Heine M, Becker AJ, Schoch S. Calcium channel subunit α2σ4 is regulated by early growth response 1 and facilitates epileptogenesis. J. Neurosci. Society for Neuroscience, 2019; 39: 3175–3187

Malter MP, Helmstaedter C, Urbach H, Vincent A, Bien CG. Antibodies to glutamic acid decarboxylase define a form of limbic encephalitis. Ann. Neurol. Ann Neurol, 2010; 67: 470–478

Matsumoto N, Hori I, Kajita MK, Murase T, Nakamura W, Tsuji T, Miyake S, Inatani M, Konishi Y. Intermitochondrial signaling regulates the uniform distribution of stationary mitochondria in axons. Mol. Cell. Neurosci. Mol Cell Neurosci, 2022; 119

McKeon A, Tracy JA. GAD65 neurological autoimmunity. Muscle Nerve. Muscle Nerve, 2017; 56: 15–27

Müller CS, Bildl W, Haupt A, Ellenrieder L, Becker T, Hunte C, Fakler B, Schulte U. Cryo-slicing blue native-mass spectrometry (csBN-MS), a Novel technology for high resolution complexome profiling. Mol. Cell. Proteomics. 2016; 15: 669–681

Müller CS, Haupt A, Bildl W, Schindler J, Knaus HG, Meissner M, Rammner B, Striessnig J, Flockerzi V, Fakler B, Schulte U. Quantitative proteomics of the Cav2 channel nanoenvironments in the mammalian brain. Proc. Natl. Acad. Sci. U. S. A. 2010; 107: 14950–14957

Nakagami Y, Sugihara G, Nakashima N, Hazama M, Son S, Ma S, Matsumoto R, Murai T, Ikeda A, Murakami K. Anti-PDHA1 antibody is detected in a subset of patients with schizophrenia. Sci Rep. Sci Rep, 2020; 10: 7906

Palmer JM, Yeaman SJ, Bassendine MF, James OFW. M4 and M9 autoantigens in

primary biliary cirrhosis--a negative study. J. Hepatol. J Hepatol, 1993; 18: 251–254

Patel MS, Korotchkina LG, Sidhu S. Interaction of E1 and E3 components with the core proteins of the human pyruvate dehydrogenase complex. J. Mol. Catal. B Enzym. J Mol Catal B Enzym, 2009; 61: 2–6

Patel MS, Nemeria NS, Furey W, Jordan F. The pyruvate dehydrogenase complexes: structure-based function and regulation. J. Biol. Chem. J Biol Chem, 2014; 289: 16615–16623

Pisetsky DS, Spencer DM, Mobarrez F, Fuzzi E, Gunnarsson I, Svenungsson E. The Binding of SLE Autoantibodies to Mitochondria. Clin. Immunol. NIH Public Access, 2020; 212: 108349

Pitsch J, Kamalizade D, Braun A, Kuehn JC, Gulakova PE, Rüber T, Lubec G, Dietrich D, von Wrede R, Helmstaedter C, Surges R, Elger CE, Hattingen E, Vatter H, Schoch S, Becker AJ. Drebrin Autoantibodies in Patients with Seizures and Suspected Encephalitis. Ann. Neurol. John Wiley and Sons Inc., 2020; 87: 869–884

von Podewils F, Suesse M, Geithner J, Gaida B, Wang ZI, Lange J, Dressel A, Grothe M, Kessler C, Langner S, Runge U, Bien CG. Prevalence and outcome of late-onset seizures due to autoimmune etiology: A prospective observational population-based cohort study. Epilepsia. Blackwell Publishing Inc., 2017; 58: 1542–1550

Poyatos E, Morandeira F, Climent J, Mas V, Castellote J, Bas J. Detection of anti-mitochondrial 2-oxoacid dehydrogenase complex subunit’s antibodies for the diagnosis of primary biliary cholangitis. Clin. Immunol. Academic Press, 2021; : 108749

Quertermous T. Plating and transferring bacteriophage libraries. Curr. Protoc. Mol. Biol. Curr Protoc Mol Biol, 2001; Chapter 6

Rangaraju V, Calloway N, Ryan TA. Activity-driven local ATP synthesis is required for synaptic function. Cell. Cell, 2014; 156: 825–835

Rigopoulou EI, Bogdanos DP. Role of autoantibodies in the clinical management of primary biliary cholangitis. 2023; 29: 1795–1810

Roberts RC. Postmortem studies on mitochondria in schizophrenia. Schizophr. Res. Elsevier B.V., 2017; 187: 17–25

La Rosa L, Covini G, Galperin C, Catelli L, Del Papa N, Reina G, Morabito A, Balestrieri G, Tincani A, Gershwin ME, Meroni PL. Anti-mitochondrial M5 type antibody represents one of the serological markers for anti-phospholipid syndrome distinct from anti-cardiolipin and anti-β2-glycoprotein I antibodies. Clin. Exp. Immunol. Oxford University Press, 1998; 112: 144

Safiulina D, Kaasik A. Energetic and dynamic: how mitochondria meet neuronal energy demands. PLoS Biol. PLoS Biol, 2013; 11

Scharf M, Miske R, Kade S, Hahn S, Denno Y, Begemann N, Rochow N, Radzimski C, Brakopp S, Probst C, Teegen B, Stöcker W, Komorowski L. A spectrum of neural autoantigens, newly identified by histo-immunoprecipitation, mass spectrometry, and recombinant cell-based indirect immunofluorescence. Front. Immunol. Frontiers Media S.A., 2018; 9

Schmidt N, Kollewe A, Constantin CE, Henrich S, Ritzau-Jost A, Bildl W, Saalbach A, Hallermann S, Kulik A, Fakler B, Schulte U. Neuroplastin and Basigin Are Essential Auxiliary Subunits of Plasma Membrane Ca2+-ATPases and Key Regulators of Ca2+ Clearance. Neuron. Elsevier Inc., 2017; 96: 827-838.e9

Schulmann A, Ryu E, Goncalves V, Rollins B, Christiansen M, Frye MA, Biernacka J, Vawter MP. Novel Complex Interactions between Mitochondrial and Nuclear DNA in Schizophrenia and Bipolar Disorder. Mol. neuropsychiatry. Mol Neuropsychiatry, 2019; 5: 13–27

Sgrignani J, Chen JJ, Alimonti A, Cavalli A. How phosphorylation influences E1 subunit pyruvate dehydrogenase: A computational study. Sci. Rep. Nature Publishing Group, 2018; 8: 14683

Shimoda S, Ishikawa F, Kamihira T, Komori A, Niiro H, Baba E, Harada K, Isse K, Nakanuma Y, Ishibashi H, Gershwin ME, Harada M. Autoreactive T-cell responses in primary biliary cirrhosis are proinflammatory whereas those of controls are regulatory.

Gastroenterology. Gastroenterology, 2006; 131: 606–618

Shimoda S, Van De Water J, Ansari A, Nakamura M, Ishibashi H, Coppel RL, Lake J, Keeffe EB, Roche TE, Gershwin ME. Identification and precursor frequency analysis of a common T cell epitope motif in mitochondrial autoantigens in primary biliary cirrhosis. J. Clin. Invest. J Clin Invest, 1998; 102: 1831–1840

Shuai Z, Wang J, Badamagunta M, Choi J, Yang G, Zhang W, Kenny TP, Guggenheim K, Kurth MJ, Ansari AA, Voss J, Coppel RL, Invernizzi P, Leung PSC, Gershwin ME. The fingerprint of antimitochondrial antibodies and the etiology of primary biliary cholangitis. Hepatology. Hepatology, 2017; 65: 1670–1682

Stacpoole PW, McCall CE. The pyruvate dehydrogenase complex: Life's essential, vulnerable and druggable energy homeostat. Mitochondrion. Mitochondrion, 2023; 70: 59–102

Su YC, Zagha E, Kwon ES, Ozaita A, Bobik M, Martone ME, Ellisman MH, Heintz N, Rudy B. Distribution of Kv3.3 potassium channel subunits in distinct neuronal populations of mouse brain. J. Comp. Neurol. J Comp Neurol, 2007; 502: 953–972

Tanaka A. Current understanding of primary biliary cholangitis. Clin. Mol. Hepatol. Korean Association for the Study of the Liver, 2021; 27: 1

Timbrell JA. The role of metabolism in the hepatotoxicity of isoniazid and iproniazid. Drug Metab. Rev. Drug Metab Rev, 1979; 10: 125–147

Tüzün E, Dalmau J. Limbic encephalitis and variants: Classification, diagnosis and treatment. Neurologist. 2007; 13: 261–271

Walker JG, Doniach D, Roitt IM, Sherlock S. Serological Tests in Diagnosis of Primary Biliary Cirrhosis. Lancet. 1965; 285: 827–831

Yang Y, Choi J, Chen Y, Invernizzi P, Yang G, Zhang W, Shao T hong, Jordan F, Nemeria NS, Coppel RL, Ridgway WM, Kurth M, Ansari AA, Leung PSC, Gershwin ME. E. coli and the etiology of human PBC: Antimitochondrial antibodies and spreading determinants. Hepatology. John Wiley and Sons Inc, 2022; 75: 266–279

Zhang H, Zhou C, Wu L, Ni F, Zhu J, Jin T. Are onconeural antibodies a clinical phenomenology in paraneoplastic limbic encephalitis? Mediators Inflamm. Mediators Inflamm, 2013; 2013

Zsurka G, Kunz WS. Mitochondrial dysfunction and seizures: the neuronal energy crisis. Lancet. Neurol. Lancet Neurol, 2015; 14: 956–966

9. Statement on personal Contributions

This doctoral thesis was conducted at the Institute of Neuropathology and the Department of Epileptology of the University Hospital Bonn under the supervision of Prof. Dr. Albert J. Becker and PD Dr. Julika Pitsch.

The conceptualization of the project was developed by me (doctoral candidate), PD Dr. Julika Pitsch (principal investigator), and Prof. Dr. Albert J. Becker (doctoral advisor).

All experiments, analyses, and data interpretations were carried out independently by me, following initial training by Delara Kamalizade, and with support from Annika Breuer, Dr. Tobias Baumgartner, Prof. Dr. Susanne Schoch, PD Dr. Julika Pitsch, and Prof. Dr. Albert J. Becker.

Mass spectrometry analyses were performed by Dr. Marc Sylvester at the Core Facility Analytic Proteomics of the University of Bonn. The screening of patients' biosamples for known neuronal antibodies and non-specific brain protein–reactive autoantibodies were carried out at the Encephalitis Laboratory of the Institute of Neuropathology (Prof. Dr. Albert J. Becker) as part of routine clinical diagnostics.

The sacrifice of mice and post- mortem removal of brain tissue, followed by tissue processing, was conducted at the Institute of Neuropathology by myself, Pia Trebing, and PD Dr. Julika Pitsch. Preparation of primary hippocampal neurons was performed by Sabine Opitz.

The data used for analysis were independently generated and compiled by me in collaboration with PD Dr. Julika Pitsch and Prof. Dr. Albert J. Becker. Statistical analysis was performed independently by me using GraphPad Prism 8.

All figures presented in this thesis were independently created by me using Adobe Illustrator 2021, Microsoft PowerPoint and Excel 365.

To improve the readability and language of the manuscript, I used ChatGPT and Copilot. After using these tools, I reviewed and revised all corresponding passages. I take full responsibility for the content of the published dissertation.

I hereby declare that I have written this thesis independently and have used no sources or aids other than those indicated.

10. Acknowledgement

I want to express my sincere gratitude to everyone who supported me during my time in the lab and while writing this thesis.

First, I want to thank all the patients who generally consented to using their biosamples for scientific research purposes. Their contribution formed the foundation of this project.

I appreciate the University of Bonn for providing me with an exceptional education that fueled my fascination for scientific problems and opened the door to the world of research. I am grateful to the BONFOR Doctoral Fellowship from the University of Bonn and the Else- Kröner- Fresenius Foundation. The funding and structural research programs provided by these scholarships were crucial to the success of this project.

Special thanks go to my mentors and doctoral advisors, Prof. Dr. Albert J. Becker and PD Dr. Julika Pitsch. Their passion for scientific and neuroimmunological questions in the field of autoimmune diseases was truly inspiring. I am deeply thankful for the trust they placed in me, their continuous support in pursuing a scientific career, and their profound expertise and guidance throughout this journey.

I like to thank the entire Becker-Pitsch research group, especially Pia Trebing and Sabine Opitz for their invaluable assistance with laboratory techniques.

My thank also goes to Prof. Dr. Volkmar Gieselmann and Dr. Marc Sylvester from the Institute of Biochemistry and Molecular Biology, University of Bonn for the excellent collaboration on mass spectrometric analyses, which significantly contributed to the success of this project.

Finally, I want to apologize to my family and friends whom I often overlooked while working on this project but without whom nothing is worth achieving. I am deeply grateful for their understanding and incredible support.